Polarization phenomena in x-ray optics

V. A. Belyakov and V. E. Dmitrienko

All-Union Scientific Research Center for the Study of the Properties of Surfaces and Vacuum

Usp. Fiz. Nauk **158**, 679–721 (August 1989)

This review is devoted to polarization phenomena observed in the x-ray range. It is noted that x-ray polarization effects are due to two physical factors, namely, the diffraction of x-rays and the anisotropy of the x-ray susceptibility of atoms in crystals. Diffraction-induced birefringence, dichroism, and change in polarization state are very dependent on the degree of imperfection of the crystal. Effects associated with the anisotropy of x-ray susceptibility, which have not been adequately investigated so far, are discussed in some detail. The anisotropy can lead to a qualitatively new effect, namely, the appearance of additional reflections with unusual polarization properties that provide information about crystal structure and chemical bonding. Magnetic scattering of synchrotron x-rays has become a powerful tool for the investigation of magnetic ordering in crystals. Practical applications discussed in this review include different modern x-ray polarizers, analyzers, and quarter-wave plates for obtaining and analyzing circular polarizations.

Introduction. X-ray optics has been going through a veritable renaissance in recent years because of improvements in instrumentation and methods of measurement, which has been partly but not entirely due to the availability of synchrotron sources of radiation. One of the interesting phenomena in the development of x-ray optics has been the study of polarization effects. As far back as 1906, the polarization of x-rays scattered through 90° was used to demonstrate their electromagnetic character.[1] Classical phenomena, such as birefringence, dichroism, and rotation of the plane of polarization,[2–6] have been observed in x-ray optics and there have been discussions of the possibility of producing quarter-wave plates capable of transforming linear into circular polarization and vice versa.[3,7–9]

It is important to emphasize that, whereas in ordinary optics, dealing with visible radiation, the wavelength is much greater than the interatomic separation, in x-ray optics the phenomenon of Bragg diffraction has a significant influence on the optical characteristics of a crystal. For example, the contribution of Bragg diffraction to dichroism, birefringence, and the transformation of polarization can sometimes be the dominant factor. In particular, it is interesting to note that diffractive birefringence, essentially a spatial dispersion effect, is observed not only in low-symmetry crystals, but even in cubic crystals. Diffractive polarization phenomena are aleady being used to investigate imperfections in crystals,[10–14] where the complete description of such phenomena necessitates the use of the dispersion equation for the polarization tensors of x-ray beams[15] by analogy with the tensors used in the theory of radiation transfer in random media.[16–19]

It is important to note that polarization phenomena due to the anisotropy of the x-ray susceptibility of crystals are relatively weak and mostly observed near the absorption edges, i.e., in regions in which effects associated with the chemical binding of electrons in atoms are significant. Very recently, it has been shown that the anisotropy of x-ray susceptibility leads to a qualitatively new effect, namely the appearance of additional diffraction maxima with unusual polarization properties, containing information about the structure of crystals and chemical bonds of atoms in crystals.[20–23 1)] Particularly interesting and promising is the magnetic scattering of x-rays,[24–28] which is due to the weak dependence of the x-ray scattering amplitude on the magnetic moment of the atom. It varies in important and informative ways with the polarization parameters. Because of improvements in x-ray diffraction studies and the increasing availability of new high-intensity x-ray sources, it is expected[26,27] that magnetic scattering will become a working method for the direct determination of the magnetic structure of crystals, especially their surface layers, and may well compete with magnetic neutron-diffraction studies.

This review consists of two sections devoted to the theory of polarization effects and a section devoted to applications, although many of the latter are discussed in the first two sections as well. We analyze and generalize an extensive range of factual material scattered among numerous publications, but we devote particular attention to the possible applications of x-ray polarization methods to the study of the structure and properties of solids. There is no doubt that this subject will advance in the next few years, especially in connection with the advent of specialized sources of synchrotron radiation, including those that will be available in our country. Polarization measurements are also topical for x-ray astronomy, but this aspect of the subject is outside the scope of the present review.

1. Polarization phenomena in diffraction. X-ray diffraction by crystals is one of the basic methods of studying the crystalline structure of matter, and is widely used in x-ray optics. For example, diffraction monochromators and spectrometers are used to produce, transform, and analyze x-ray beams. In this Section, we shall examine in detail the change in the polarization of primary and diffracted beams during diffraction. We shall concentrate our attention on topics that are of current interest, e.g., diffractive birefringence and dichroism, and the change of polarization state on diffraction in perfect and imperfect crystals. We emphasize that, in contrast to Sec. 2, we shall adopt the traditional ap-

 0038-5670/89/080697-23$01.80

proach in this section and assume that the x-ray susceptibility is isotropic in order to isolate polarization phenomena that originate in pure Bragg diffraction.

1.1. Diffraction in perfect crystals (kinematic and dynamic theories). The diffraction of x-rays by perfect crystals has been discussed in an enormous number of papers (see, for example, Refs. 29–32), so that we shall confine ourselves to a brief description of the basic results with particular reference to the polarization characteristics of diffracted beams. The radiation field inside and outside a crystal is found by solving the Maxwell equations with appropriate boundary conditions. The permittivity of the crystal is described by the three-dimensional periodic tensor

$$\hat{\varepsilon}(\mathbf{r}) = 1 + \hat{\chi}(\mathbf{r}) = 1 + \sum_{\mathbf{H}} \hat{\chi}_{\mathbf{H}} \exp(i\mathbf{H}\mathbf{r}), \tag{1.1}$$

where $\hat{\chi}(r)$ is the permittivity of the crystal in the x-ray range, $\hat{\chi}_{\mathbf{H}}$ are the Fourier harmonics of the x-ray susceptibility, and $\mathbf{H}$ is the reciprocal lattice vector of the crystal. If the susceptibility is isotropic, all the $\hat{\chi}_{\mathbf{H}}$ are proportional to a unit tensor: $(\hat{\chi}_{\mathbf{H}})_{ik} \equiv \chi_{\mathbf{H}} \delta_{ik}$, where

$$\chi_{\mathbf{H}} = -\frac{r_e \lambda^2}{\pi V} F_{\mathbf{H}}. \tag{1.2}$$

In this expression, $r_e = e^2/mc^2$ is the classical radius of the electron, λ is the wavelength, V is the volume of the unit cell, and $F_{\mathbf{H}}$ is the structure amplitude corresponding to the reflection $\mathbf{H}$ (Refs. 29–32) (for $\lambda \sim 1$ Å, we find that $|\chi_{\mathbf{H}}| \lesssim 10^{-5}$).

Maxwell's equations with permittivity given by (1.1) can be solved analytically only by adopting some particular approximation. We shall usually employ the two-wave approximation (with the exception of Sec. 1.3). It is assumed in this approximation that only two waves have appreciable intensity, namely, the direct wave and one diffracted wave, i.e., Bragg's condition is satisfied only for a single reciprocal lattice vector $\mathbf{H}$. In general, there will be several diffracted waves, but multiple-wave diffraction is rare because stringent geometric conditions are imposed on the direction of propagation of the primary wave for a given wavelength. The characteristic feature of the two-wave approximation is the independent diffraction scattering of σ and π polarized waves [$\sigma(\pi)$ polarization is the linear polarization for which the electric field vector is orthogonal (parallel) to the plane of scattering formed by the wave vectors $\boldsymbol{\kappa}_0$ and $\boldsymbol{\kappa}_{\mathbf{H}} = \boldsymbol{\kappa}_0 + \mathbf{H}$ of the direct and diffracted waves, respectively].

Crystal field amplitudes can be calculated within the framework of the two-wave approximation by either kinematic or dynamic theory of diffraction. In the kinematic theory, the crystal is assumed to be so thin that we need only take into account single diffraction scattering (the Born approximation), whereas, in dynamic theory, the multiple scattering of incident into diffracted waves and vice versa is taken into account, especially in thick crystals. The characteristic parameter that can be used to distinguish thick from thin perfect crystals is the primary extinction length

$$L_e^I = \frac{\lambda}{|\chi_{\mathbf{H}}|}.$$

The kinematic theory is valid when the distances traversed in the crystal by both the incident and diffracted waves are much shorter than the primary extinction length ($L_e^I \gtrsim 10$ μm for $\lambda \sim 1$ Å). The polarization properties of diffraction are found to be particularly simple in the kinematic theory in which the scattering amplitudes for σ and π polarized waves differ by the polarization factor $\cos 2\Theta$, where 2Θ is the scattering angle (the angle between $\boldsymbol{\kappa}_0$ and $\boldsymbol{\kappa}_{\mathbf{H}}$) and

$$E_\sigma^d = AF_{\mathbf{H}} E_\sigma^i, \qquad E_\pi^d = AF_{\mathbf{H}} E_\pi^i \cos 2\Theta, \tag{1.3}$$

in which $E_{\sigma,\pi}^i$ and $E_{\sigma,\pi}^d$ are the components of the incident and diffracted waves, respectively, and the factor A depends on the diffraction geometry, wavelength, and deviation $\Delta\Theta = \Theta - \Theta_B$ of the angle of incidence Θ from the Bragg angle Θ_B. The significant point is that the factor A does not affect the polarization properties of kinematic diffraction, and its specific form for a crystal in the form of a plane-parallel plate can be obtained from the formulas of the dynamic theory, given below, by going to the limit of a very small thickness.[29] Since the angle Θ changes by a very small amount $\Delta\Theta \lesssim 10^{-4}$ in the diffraction region, the polarization factor in (1.3) can be replaced with $\cos 2\Theta_B$. The expressions given by (1.3) are conveniently written in the vector form $\mathbf{E}^d = \hat{R}_k \mathbf{E}^i$, where the scattering matrix is given by

$$\hat{R}_k = AF_{\mathbf{H}} \begin{pmatrix} 1 & 0 \\ 0 & \cos 2\Theta_B \end{pmatrix} = AF_{\mathbf{H}} \hat{K}. \tag{1.4}$$

The particular feature of the kinematic case is that the polarization of the diffracted wave is determined by the ratio E_π^d/E_σ^d, which is constant throughout the diffraction region. In particular, σ and π polarized incident beams produce σ and π polarized diffracted beams: linearly polarized incident beams produce linearly polarized diffracted beams independently of the angle of incidence; the sign of elliptic polarization changes on diffraction if $\cos 2\Theta_B < 0$, but does not change when $\cos 2\Theta_B > 0$; for scattering through 90°, the diffracted wave is σ polarized.

The polarization properties are much more complicated in the dynamic theory than in the kinematic theory. The physical reason for this is that the width of the diffraction region is different for the σ and π polarizations and, moreover, the relative phase of the σ and π components of the diffracted waves undergoes a change in the diffraction region. It is well known[29–32] that four Bloch waves (two σ polarized and two π polarized) are produced in a perfect crystal, and each has its own wave vector. The characteristic difference between these wave vectors is of the order of $1/L_e^I$ and interference between the Bloch waves gives rise to nontrivial polarization properties. The solution of the dynamic diffraction problem for a plane-parallel plate leads to the following expressions for the amplitudes of diffracted and transmitted waves:

$$E_\sigma^d = R_{\sigma\sigma} E_\sigma^i, \quad E_\pi^d = R_{\pi\pi} E_\pi^i, \tag{1.5}$$

$$E_\sigma^t = T_{\sigma\sigma} E_\sigma^i, \quad E_\pi^t = T_{\pi\pi} E_\pi^i. \tag{1.6}$$

The coefficients $R_{\gamma\gamma}$ and $T_{\gamma\gamma}$ ($\gamma = \sigma,\pi$) in (1.5) and (1.6) are given by the following expressions:

(a) The Bragg case (the incident and diffracted waves leave through the same surfaces of the plate):

$$R_{\gamma\gamma} = \chi_H C_\gamma (\alpha + i\Delta_\gamma \operatorname{ctg} l_\gamma)^{-1},$$

$$T_{\gamma\gamma} = (\cos l_\gamma - i\alpha\Delta_\gamma^{-1} \sin l_\gamma)^{-1} \exp\left[i\varkappa_0^2 L\,(\chi_0 - \alpha b)\,(2\varkappa_0 s)^{-1}\right] \tag{1.7}$$

(b) The Laue case (incident and diffracted waves leave through different surfaces of the plate):

$$R_{\gamma\gamma} = \chi_H C_\gamma \Delta_\gamma^{-1} \sin l_\gamma \exp\left[i\varkappa_0^2 L\,(\chi_0 - \alpha b)\,(2\varkappa_0 s)^{-1}\right],$$

$$T_{\gamma\gamma} = (\cos l_\gamma + i\alpha\Delta_\gamma^{-1} \sin l_\gamma) \exp\left[i\varkappa_0^2 L\,(\chi_0 - \alpha b)\,(2\varkappa_0 s)^{-1}\right], \tag{1.8}$$

where

$$\alpha = \frac{\mathbf{H}^2 + 2\varkappa_0 \mathbf{H}}{2\varkappa_0^2} + \frac{\chi_0 (1-b)}{2b},$$

$$\Delta_\gamma = \left(\alpha^2 + \frac{C_\gamma^2 \chi_H \chi_{\bar{H}}}{b}\right)^{1/2},$$

$$l_\gamma = \frac{\Delta_\gamma \varkappa_0^2 L}{2\varkappa_H s}, \quad b = \frac{\varkappa_0 s}{\varkappa_H s},$$

$C_\sigma = 1, C_\pi = \cos 2\Theta_B$, and $\mathbf{s}$ is the inward normal to the entrance surface of the sample. The parameter α can be expressed in terms of the deviation of the angle of incidence from the Bragg angle:

$$\alpha = (\Theta_B - \Theta) \sin 2\Theta_B + \frac{\chi_0 (1-b)}{2b}. \tag{1.9}$$

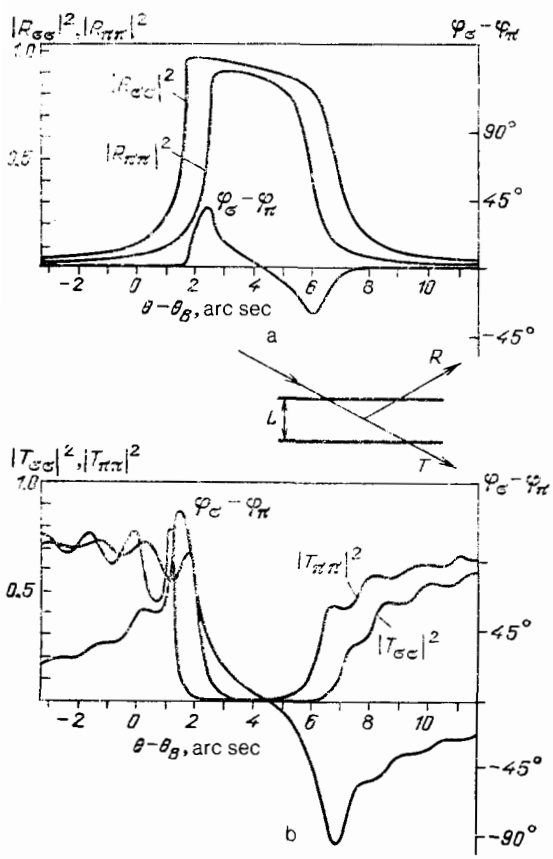

FIG. 1. a—Reflection coefficients $|R_{\sigma\sigma}|^2, |R_{\pi\pi}|^2$ and the difference $\varphi_\sigma - \varphi_\pi$ between diffraction corrections to the σ and π polarized waves in the symmetric Bragg case; 220 reflection in Si, semi-infinite crystal, CuK_α radiation. b—Transmission coefficients $|T_{\sigma\sigma}|^2, |T_{\pi\pi}|^2$ and the difference $\varphi_\sigma - \varphi_\pi$ between diffraction corrections to the phase of σ and π polarized transmitted waves in the symmetric Bragg case; 220 reflection in Si, $L = 10\,\mu$m, CuK_α radiation; dashed line corresponds to the transmission coefficient in the absence of diffraction. Insert shows the diffraction geometry.

Formulas (1.5)–(1.9) can be used to perform a full analysis of polarization phenomena in perfect crystals. In particular, it follows from them that the amplitude and relative phase of diffracted waves with σ and π polarizations undergo a variation within the diffraction region (Figs. 1a and 2a). Usually, the reflection coefficient $|R_{\gamma\gamma}|^2$ for σ polarization is greater than for π polarization, but the reverse situation is also possible because of the so-called pendellösung that arises as a consequence of interference between the two Bloch functions associated with each polarization state.

The amplitude and phase of the waves transmitted by the crystal (see Figs. 1b and 2b) also undergo changes within the diffraction region, which can be described as the manifestation of an effective diffractive birefringence and dichroism (see Sec. 1.3).[2)] We emphasize that this dichroism is related exclusively to the difference between the absorption of radiation of different polarization (as in ordinary optics) and, in the first instance, the difference between the diffracted intensities of σ and π polarized waves. As far as true absorption is concerned, this can be significant for dichroism under the conditions of anomalous absorption (Borrmann effect), which is also used to produce polarized beams (Sec. 3.2).

1.2 Polarization tensor and integrated polarization parameters. In practice, one frequently has to deal with the description of partially polarized beams. X-ray sources usually produce either partially polarized or completely unpolarized radiation. It will be seen below that a change in the polarization state occurs when the polarization parameters

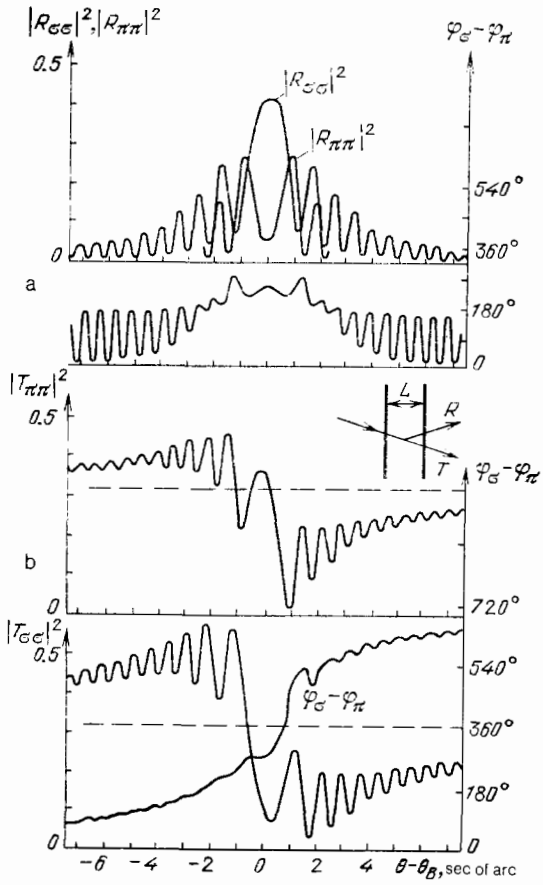

FIG. 2. Same as Fig. 1 but for the symmetric Laue case. $L = 72\,\mu$m.

TABLE I. Polarization parameters of beams $z = E_\pi/E_\sigma$.

Parameter	Polarization	
	total	partial
1. Intensity I	$\lvert E_\sigma\rvert^2 + \lvert E_\pi\rvert^2$	$J_{\sigma\sigma} + J_{\pi\pi}$
2. Degree of polarization P	1	$\dfrac{[(J_{\sigma\sigma} - J_{\pi\pi})^2 + 4\lvert J_{\sigma\pi}\rvert^2]^{1/2}}{J_{\sigma\sigma} + J_{\pi\pi}}$
3. Ratio of axes of polarization elipse b_e	$\dfrac{-2\,\mathrm{Im}\,z}{1+\lvert z\rvert^2+[(1-\lvert z\rvert^2)^2+4(\mathrm{Re}\,z)^2]^{1/2}}$	$\dfrac{2\,\mathrm{Im}\,J_{\sigma\pi}}{PI+[(J_{\sigma\sigma} - J_{\pi\pi})^2 + 4(\mathrm{Re}\,J_{\sigma\pi})^2]^{1/2}}$
4. angle of rotation, ψ of the semi-major axis of the elipse relative to the σ polarization	$\dfrac{1}{2}\,\mathrm{arctg}\dfrac{2\,\mathrm{Re}\,z}{1-\lvert z\rvert^2}$	$\dfrac{1}{2}\,\mathrm{arctg}\dfrac{2\,\mathrm{Re}\,J_{\sigma\pi}}{J_{\sigma\sigma} - J_{\pi\pi}}$

are averaged over the diffraction region, and also in the case of diffraction by imperfect crystals. The complete description of the polarization properties and intensities of such beams is accomplished with the aid of the polarization tensor $\hat{J}$ (Refs. 15–19), defined by

$$J_{\beta\gamma} = \overline{E_\beta E_\gamma^*}, \tag{1.10}$$

where the bar indicates averaging (with respect to time in the classical language[17] or over the photon ensemble in the quantum-mechanical language[33]). In a beam with polarization tensor $\hat{J}$, the intensity of a component with arbitrary polarization represented by the unit vector $\mathbf{e}$ is given by the expression $(\mathbf{e}^*\hat{J}\mathbf{e})$. Throughout the discussion presented below, we shall always use the σ and π unit polarization vectors as our basis. The physical meaning of the elements of the tensor $\hat{J}$ in this basis is as follows: $J_{\sigma\sigma}$ and $J_{\pi\pi}$ are the intensities of the σ and π components, respectively, 2 Re $J_{\sigma\pi}$ is the intensity difference between the components that are linearly polarized at $\pm 45°$ to σ, and 2 Im $J_{\sigma\pi}$ is the intensity ratio of components with right and left circular polarizations (a total of four independent elements). The polarization tensor is convenient because, when coherent beams are combined, their polarization tensors are added. The expressions relating the intensity and the polarization parameters of a beam, on the one hand, and the components of the polarization tensors, on the other, are given in Table I. We note that the Stokes parameters[16–18] and the polarization density matrix[33] are widely used to describe partially polarized beam (all these approaches are, of course, equivalent).

The transformation formulas for the beam polarization tensor in the case of diffraction by perfect crystals can be obtained from the above formulas for the fields, as given by (1.3)–(1.8). By constructing the quadratic combinations (1.10) for the diffracted and transmitted wave fields, we obtain

$$\begin{aligned} \hat{J}^d &= \hat{R}\hat{J}^i\hat{R}^*, \\ \hat{J}^t &= \hat{T}\hat{J}^i\hat{T}^*, \end{aligned} \tag{1.11}$$

where the diagonal components of the matrices are all zero. The diagonal form of the matrices $\hat{R}$ and $\hat{T}$ leads to the fact that each of the components of the polarization tensors $\hat{J}^d$ and $\hat{J}^t$ depends only on the corresponding component of $\hat{J}^i$:

$$\begin{aligned} J^d_{\beta\gamma} &= R_{\beta\beta}R^*_{\gamma\gamma}J^i_{\beta\gamma}, \\ J^t_{\beta\gamma} &= T_{\beta\beta}T^*_{\gamma\gamma}J^i_{\beta\gamma}, \end{aligned} \tag{1.12}$$

where $\beta = \sigma, \pi$, $\gamma = \sigma, \pi$ (no summation over repeated indices!).

Formulas (1.11) and (1.12) readily explain the change in polarization and in the degree of polarization of the beam on diffraction. For example, one can use the expressions listed in Table I to show that, if $J^i_{\sigma\sigma}/J^i_{\pi\pi} \leqslant |R_{\pi\pi}|^2/|R_{\sigma\sigma}|^2$, then, for any incident-beam polarization, the degree of polarization of the diffraction beam does not increase, i.e., $P^d \leqslant P^i$. The change in the intensity and polarization of the beam on successive reflection from a number of crystals is also conveniently described by the successive application of (1.11) and (1.12). This procedure becomes nontrivial if the crystals are rotated relative to one another so that the σ and π polarizations for them are not the same. It is then necessary to transform the polarization tensors from one basis (σ, π) to another (σ', π'), where the latter is rotated relative to the former by ψ':

$$\hat{J}' = \hat{R}_{\psi'}\hat{J}\hat{R}^{-1}_{\psi'}, \tag{1.13}$$

in which the rotation matrix $\hat{R}_{\psi'}$ is given by

$$\hat{R}_{\psi'} = \begin{pmatrix} \cos\psi' & \sin\psi' \\ -\sin\psi' & \cos\psi' \end{pmatrix}. \tag{1.14}$$

The polarization tensor is also convenient in finding the integrated (over the diffraction region) polarization parameters. These are given by the integrated polarization tensors:

$$\begin{aligned} \bar{J}^d_{\beta\gamma} &= \int J^i_{\beta\gamma}R_{\beta\beta}R^*_{\gamma\gamma}\,d\Theta, \\ \bar{J}^t_{\beta\gamma} &= \int J^i_{\beta\gamma}T_{\beta\beta}T^*_{\gamma\gamma}\,d\Theta. \end{aligned} \tag{1.15}$$

It follows from (1.15) that diffraction by a thick perfect crystal, even for a completely polarized incident beam, gives rise to a degree of repolarization, provided only that the incident beam is neither σ nor π polarized. Physically, this is related to the fact that the polarizations of the diffracted and

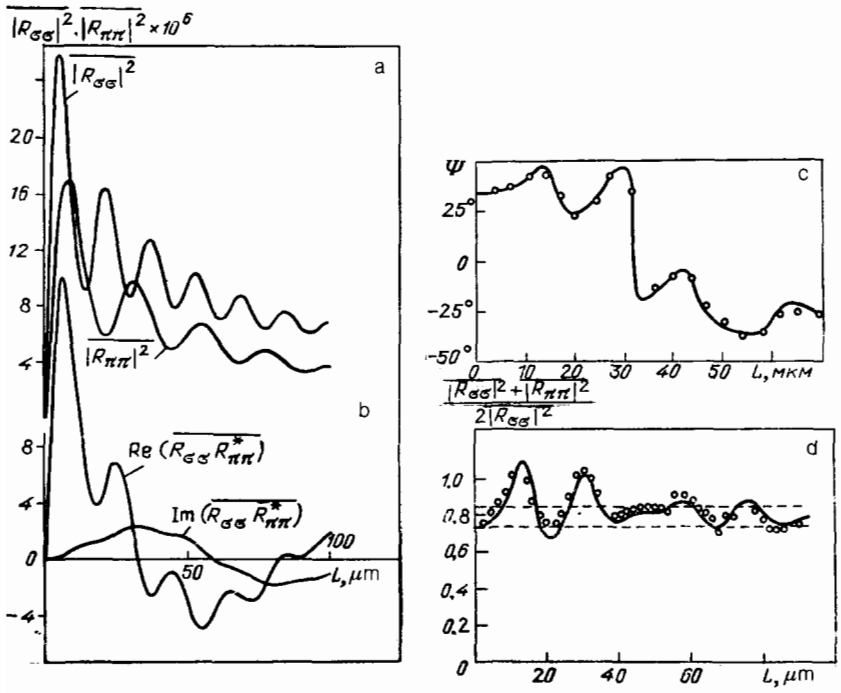

FIG. 3. Integral reflection coefficients for diagonal (a) and off-diagonal (b) components of the polarization tensor as functions of the crystal thickness. Figs. c and d, taken from Ref. 2, show the corresponding polarization parameters, i.e., rotation of the plane of polarization (c) and ratio of integral reflection coefficients for σ and π polarizations (d). Symmetric Laue case, 220 reflection in Si, CuK_α radiation. Solid curves—calculated from dynamic theory, points—experimental for linear polarization at 45° to the σ and π vectors; dashed lines correspond to $(1+\cos 2\Theta_B)/2$ and $(1+\cos^2+2\Theta_B)/2$.

transmitted waves undergo a change in the diffraction region (see Figs. 1 and 2), and the incoherent superpositions of beams with different polarizations results in partially polarized beams.

The integrated reflections coefficients and the integrated polarization parameters (Fig. 3) are oscillating functions of thickness that are related to the well-known pendellösung solutions for waves diffracted in the crystal. We note that, for certain particular thicknesses that correspond to $\mathrm{Re}\ \overline{R_{\sigma\sigma}R^*_{\pi\pi}}=0$, the diffracted beam is circularly polarized if the incident beam is linearly polarized at the angle $\Psi^i=\mathrm{arctg}(\overline{|R_{\sigma\sigma}|^2}/\overline{|R_{\pi\pi}|^2})^{0.5}$ to the direction of the σ polarization. However, the degree of circular polarization is then shown by Fig. 3 and Table I to be relatively small $P\approx 0.25$ for $L\approx 33\ \mu$m.

The use of the polarization tensors is particularly convenient in the case of imperfect crystals (Sec. 1.4).

1.3. Diffractive birefringence and dichroism. A monochromatic wave falling on a crystal produces in the diffraction region two σ and two π polarized Bloch waves, each with its own wave vector. As they propagate in the crystal, these waves interfere with one another, so that the polarization parameters of the waves transmitted and diffracted by the crystal are very complicated functions of the crystal thickness, which has often been observed experimentally (Refs. 2, 3, 34, and 36). However, in many cases, only one Bloch wave component is significant for each of the polarizations, and we have the simpler situation that is analogous to ordinary optics, except that the x-ray birefringence is diffractive in origin. For example, one such case is diffraction by thick absorbing crystals.[29]

Two further similar cases are discussed below, namely, "off-Bragg" diffractive birefringence and birefringence by mosaic crystals. The former is discussed in this Section and occurs for sufficiently large deviations from the Bragg angle ($\Delta\Theta=\Theta-\Theta_B$), so that one can neglect the intensity of the diffracted wave, which decreases relatively rapidly (as $|\Delta\Theta|^{-2}$) with increasing $|\Delta\Theta|$ [see (1.5)–(1.8)]. It will be clear from the account given below that, under these conditions, diffractive birefringence decreases slowly (as $|\Delta\Theta|^{-1}$) and, when the crystal thickness is large enough, a considerable phase difference is established between the σ and π polarized waves emerging from the crystal (Figs. 2b). Moreover, because of this slow reduction in birefringence, "off-Bragg" birefringence may include the contribution of many reflections. This problem is also examined below.

The diffraction correction Δn to the refractive index can be obtained in the two-wave approximation either directly from the Maxwell equations, using perturbation theory in which it is assumed that the amplitude of the diffracted wave is much smaller than that of the incident wave,[7–9] or from (1.6) which gives the amplitude of the transmitted wave in the limit as $|\Delta\Theta|\to\infty$. The final expression ($\gamma=\sigma,\pi$) that is valid in both Bragg and Laue cases is

$$\Delta n_\gamma=-\frac{C_\gamma^2\chi_H\chi_{\bar H}}{4\Delta\Theta\sin 2\Theta_B}. \tag{1.16}$$

The refractive index difference Δn is

$$\delta n=\Delta n_\sigma-\Delta n_\pi=-\frac{\chi_H\chi_{\bar H}\sin 2\Theta_B}{4\Delta\Theta}. \tag{1.17}$$

The range of validity of this expression is defined by the inequality $|\Delta\Theta|\gg|\chi_H|/\sin 2\Theta_B$.

The real part of Δn determines birefringence and the imaginary part the dichroism (i.e., different absorption) of σ and π polarized rays in the crystal.

We emphasize that the dichroism that follows from (1.17) is displayed by absorbing crystals only if $\mathrm{Im}\,\chi_H\chi_{\bar H}\neq 0$. Physically, it is related to the difference between the Borrmann effects for σ and π polarized waves.[29–31] We note that the usual situation in the x-ray region is described by $|\mathrm{Re}\,\delta n|\gg|\mathrm{Im}\,\delta n|$ (provided we are not too close to an absorption edge). Only the relative phase of the α and π polarized waves is then found to change during propagation.

In the many-wave case, the solution of the Maxwell equations can also be obtained by perturbation theory.[5,7,9] The solution is sought in the form of the Bloch wave (in this case, it is more convenient to use the induction **D**):

$$\mathbf{D}(\mathbf{r}) = \left(\mathbf{D}_0 + \sum_{\mathbf{H}\neq 0} \mathbf{D}_{\mathbf{H}} e^{i\mathbf{H}\mathbf{r}}\right) e^{i\mathbf{K}_0\mathbf{r}}. \tag{1.18}$$

Substituting this into the Maxwell equations, we obtain, as usual,[31] the set of equations of multiwave dynamic theory of diffraction. Since we cannot tell in advance which polarizations will be intrinsic, let us write this set in vector form in the case of the direct wave $\mathbf{D}_0$:

$$\left(1 - \frac{\varkappa_0^2}{K_0^2} - \chi_0\right)\mathbf{D}_0 = \sum_{\mathbf{H}\neq 0} \chi_{\bar{\mathbf{H}}}\left[\mathbf{D}_{\mathbf{H}} - \frac{\mathbf{K}_0\,(\mathbf{D}_{\mathbf{H}}\mathbf{K}_0)}{K_0^2}\right], \tag{1.19a}$$

$$\left(1 - \frac{\varkappa_0^2}{K_H^2} - \chi_0\right)\mathbf{D}_{\mathbf{H}} = \sum_{\mathbf{G}\neq\mathbf{H}} \chi_{\mathbf{H}-\mathbf{G}}\left[\mathbf{D}_{\mathbf{G}} - \frac{\mathbf{K}_{\mathbf{H}}\,(\mathbf{D}_{\mathbf{G}}\mathbf{K}_{\mathbf{H}})}{K_H^2}\right]. \tag{1.19b}$$

($\mathbf{H}\neq 0, \mathbf{K}_{\mathbf{H}} = \mathbf{K}_0 + \mathbf{H}$). Assuming that all the $\mathbf{D}_{\mathbf{H}}$ are small, and retaining only $\mathbf{D}_0$ on the right-hand side of (1.19b), we find that

$$\mathbf{D}_{\mathbf{H}} = \chi_{\mathbf{H}}\left[\mathbf{D}_0 - \frac{\mathbf{K}_{\mathbf{H}}\,(\mathbf{D}_0\mathbf{K}_{\mathbf{H}})}{K_H^2}\right]\left(1 - \frac{\varkappa_0^2}{K_H^2} - \chi_0\right)^{-1}. \tag{1.20}$$

Substituting $\mathbf{D}_{\mathbf{H}}$ in (1.19a), we obtain the following equation for the wave vector amplitudes in the crystal:

$$\left(1 - \frac{\varkappa_0^2}{K_0^2} - \chi_0 + 2\hat{\delta}^{\mathrm{d}}\right)\mathbf{D}_0 = 0, \tag{1.21}$$

where the tensor $\hat{\delta}^d$ is given by (see also Refs. 5 and 9)

$$\delta_{ik}^{\mathrm{d}} = \frac{1}{4}\sum_{\mathbf{H}\neq 0} \frac{\chi_{\mathbf{H}}\chi_{\bar{\mathbf{H}}}}{\alpha_{\mathbf{H}}\varkappa_0^2}\,(K_{\mathbf{H}}^2\delta_{ik} - H_i'H_k'), \tag{1.22}$$

and the quantity $\alpha_{\mathbf{H}} = [\mathbf{H}^2 + 2(\boldsymbol{\kappa}_0\mathbf{H})]/2\kappa_0^2$ determines the deviation of the direction of propagation of the wave $\mathbf{D}_0$ from the Bragg direction for the reflection **H**, where $\mathbf{H}' = \mathbf{H} - \boldsymbol{\kappa}_0(\boldsymbol{\kappa}_0\mathbf{H})/\kappa_0^2$.

By diagonalizing the tensor $\hat{\delta}^d$ we can find the eigenvectors $\mathbf{e}_m$ ($m = 1,2,$) and the eigenvalues δ_m^d of (1.21), which determine the polarization and the wave vector of eigenwaves in the crystal, respectively. The refractive index difference between the eigenwaves is given by $\delta n = \delta_1^d - \delta_2^d$.

We note that, for absorbing crystals, the eigenpolarizations can be elliptic and nonorthogonal, i.e., $(\mathbf{e}^*{}_1\mathbf{e}_2) \neq 0$, and the quantities δ_m^d are complex. It also follows from (1.12) that, in this particular approximation, there is neither birefringence nor dichroism for beams propagating along threefold or higher-order symmetry axes.

As an example, let us consider the propagation of x-rays at right-angles to the (110) plane in a cubic crystal. Symmetry considerations then show immediately that the eigenpolarizations are linear and one of them ($\mathbf{e}_1$) is parallel to the [001] direction, whereas the other ($\mathbf{e}_2$) is parallel to the [1$\bar{1}$0] direction. Once we know $\mathbf{e}_m$, we can readily determine δ_m^d since

$$\delta_m^{\mathrm{d}} = (\mathbf{e}_m^*\hat{\delta}^{\mathrm{d}}\mathbf{e}_m) \tag{1.23}$$

($\mathbf{e}_m$ are unit vectors). For the present case (1.22) then leads to the following expression:

$$\delta n = \sum_{h^2+k^2+l^2\neq 0}{}' \frac{[(h-k)^2 - 2l^2]\,\chi_{hkl}\chi_{\bar{h}\bar{k}\bar{l}}}{4\,[h^2 + k^2 + l^2 - (\sqrt{2}\,a/\lambda)\,(h+k)]}, \tag{1.24}$$

where a is the size of the unit cell and h, k, l are the Miller indices.

Let us now analyze the application of the general relations given by (1.22) and (1.24) and the resulting estimate of the effects for the special case of propagation of CuKα_1 radiation in silicon. Since, in this case, $\sqrt{2}a/\lambda = 4.9855 \approx 5$, the main contribution to Δn is provided by the 620 and 260 reflections, since the denominator in (1.24) is very small for these reflections. When these reflections alone are taken into account, we have $\delta n = (1.9 + i0.24)\cdot 10^{-9}$, whereas the inclusion of the remaining reflections yields $\delta n = (2.5 + i0.27)\cdot 10^{-9}$, i.e., distant reflections provide a relatively appreciable contribution. When the crystal thickness is $L \approx 0.04$ cm, the rotation $\Delta\Psi$ of the plane of polarization and the ratio b_e of the axes of the polarization ellipse are found to be measurable by existing experimental techniques[3,5] (for example, $\Delta\Psi = 3.8'$ and $b_e = 0.02$ for an incident wave polarized at 45° to the σ and π directions).

An experimental study[37] of the above case of the propagation of CuKα_1 radiation in silicon showed that both birefringence and dichroism were substantially greater than indicated by the above theoretical values. This discrepancy may be due to the fact that appreciable 260 and 620 reflections were produced in the course of collimation of the beam employed in Ref. 37. Diffraction and the Borrmann effect associated with these reflections could have given rise to a substantial increase in the observed dichroism and birefringence as compared with the theoretical predictions. These suggestions are consistent with the fact that, when measurements were performed on the same crystal but with special steps taken to exclude the 260 and 620 reflections,[5] this gave rise to significantly smaller effects than those reported in Ref. 37 (see also Ref. 38).

We therefore conclude that crystals exhibit appreciable birefringence and dichroism in the x-ray region even for directions well away from the directions of strong diffraction scattering. In contrast to the case of strong diffraction scattering, the propagation of x-rays in such cases can be described by analogy with the ordinary optics of anisotropic media, provided the diffraction terms discussed above are taken into account in the refractive index. Specific estimates (Sec. 3.3) show that the off-Bragg diffractive birefringence can be used as a basis for the transformation of linearly polarized waves into circularly polarized waves and vice versa. On the other hand, diffractive birefringence and dichroism may impede the observation of the true anisotropy of x-ray susceptibility. Diffraction corrections to the refractive index can also be very significant in precision measurements of the refractive index (using x-ray interferometers, etc.), in which a relative precision of the order of 10^{-9}–10^{-10} has already been attained.

1.4. Diffraction in imperfect crystals. The imperfection of a crystal, i.e., departure from the regular crystal lattice, ensures that waves diffracted at different points in the crystal acquire an additional phase difference. When these irregularities are random, the waves become partially incoherent because of the randomness of the phase difference. It is clear that this incoherence will affect, in the first instance, the polarization properties of diffracted waves and, in partic-

ular, can give rise to changes of polarization state. There is, at present, no theory that can describe diffraction by a crystal with arbitrary imperfections. Existing theoretical approaches apply to slightly or higher imperfect crystals. In this section, we examine only one of the simplest models, i.e., that of the mosaic crystal, which will, nevertheless, exhibit many of the polarization effects that are specific to imperfect crystals. In this model, the crystal imperfection is assumed to be so strong that waves diffracted by different blocks of the mosaic are completely incoherent, and the kinematic approximation is applied to each such block.[29,39–41]

Diffraction by mosaic crystals is traditionally discussed on the basis of the Darwin transfer equations for the intensities of the σ and π polarized components.[39–41] For beams of arbitrary polarization, the equations for the intensities must be replaced with the transfer equations for the polarization tensor $\hat{J}$ (see Sec. 1.2 for a definition of this tensor). It will be seen below that this generalization is equivalent to adding to the Darwin equations, which describe the diagonal components of the polarization tensors, a further set of equations for the off-diagonal components. Their general solution provides a complete description of the polarization properties of beams diffracted by mosaic crystals.[15]

The derivation of the transfer equations for the polarization tensor can be illustrated by the following simple argument. Consider the evolution of the polarization tensor of the direct wave $\hat{J}^0$ as it propagates in the crystal, i.e., let us find the derivative $\partial\hat{J}^0/\partial S_0$ (s_0 is the distance along the direction of propagation of the direct wave). First, we must take into account absorption that is present even outside the diffraction region, whose contribution to the derivative has the form $\mu\hat{J}^0$, where μ is the absorption coefficient. Diffraction of the diffracted wave back into the direct wave is described in precisely the same way as the diffraction of the direct wave [see (1.3), (1.4), and (1.11)] and leads to a contribution of the form $\sigma_{0\mathbf{H}}\hat{K}\hat{J}^{\mathbf{H}}\hat{K}$ to the required derivative, where $\hat{J}^{\mathbf{H}}$ is the polarization tensor of the diffracted wave and $\sigma_{0\mathbf{H}}$ is the mean Bragg scattering cross section per unit volume of the crystal for a given angular deviation $\Delta\Theta = \Theta - \Theta_B$ from the Bragg angle:

$$\sigma_{0\mathbf{H}} = \frac{\pi^2}{\lambda \sin 2\Theta_B} |\chi_{\mathbf{H}}|^2 W(\Delta\Theta) \equiv QW(\Delta\Theta). \tag{1.25}$$

The function $W(\Delta\Theta)$ in (1.25) describes the orientation distribution of the mosaic blocks. In deriving (1.25), it is assumed that the characteristic size L_b of these blocks is much less than L_e^I, so that the kinematic approximation is valid for the individual blocks and the characteristic block disorientation angle $\Delta\Theta_b$ is much less than λ/L_b (the so-called type I mosaic structure[40]).

The terms describing the change in the polarization tensor of the direct beam due to loss by diffraction have the most nontrivial form. Apart from the obvious diffractive reduction in the beam, there is an unavoidable change in the phase velocity (refractive index) in the diffraction region due to the weakening of the beam by the dispersion relations.[15] Here, the situation is analogous to the case of ordinary resonance absorption that necessarily leads to a change in the real part of the refractive index. We therefore make a small digression and consider the determination of the diffraction correction to the refractive index in an imperfect crystal.

The most systematic approach is to evaluate Δn_γ in terms of the forward scattering amplitude of an individual mosaic block (of arbitrary shape),[42] followed by averaging over block orientations. If, as assumed above, $L_b \ll L_e^I$ and $\Delta\Theta_b \gg \lambda/L_b$, we need not consider the dependence on the shape and dimensions of blocks, and we obtain the following expression for Δn_γ:

$$\Delta n_\gamma = \frac{\pi C_\gamma^2 \chi_{\mathbf{H}}\chi_{\bar{\mathbf{H}}}}{4\sin 2\Theta_B}\left(\tilde{W}(\Delta\Theta) + iW(\Delta\Theta)\right), \tag{1.26}$$

where $C_\sigma = 1, C_\pi = \cos 2\Theta_B$ and the function $\tilde{W}(\Delta\Theta)$ is related to $W(\Delta\Theta)$ by the dispersion relation

$$\tilde{W}(\Delta\Theta) = \frac{1}{\pi}\int_{-\infty}^{\infty} \frac{W(x)\,dx}{x - \Delta\Theta}. \tag{1.27}$$

This result is unusual because it involves an integral with respect to the angle of incidence and not the radiation frequency. This replacement is possible because the frequency and the angle $\Delta\Theta$ are proportional to one another by virtue of the Bragg condition (with the exception of the case $\Theta_B = 90°$!).

The relation given by (1.26) can be obtained in other ways as well. For example, if we neglect absorption, we can conclude from the law of conservation of energy that $\mathrm{Im}(\Delta n_\gamma) = \lambda\sigma_{0\mathbf{H}} C_\gamma^2/4\pi$ [see (1.25)], i.e., whatever was lost from one beam was gained by the other, and then obtain $\mathrm{Re}(\Delta n_\gamma)$ with the aid of the dispersion relations. Another method[42] consists of evaluating Δn_γ from the amplitude of the wave transmitted by the crystal [see (1.6)] in the limit of very thin flat mosaic blocks, followed by averaging over the orientations of the individual blocks. The dispersion relations given by (1.27) are obtained automatically in this approach.

We note that (1.26) enables us correctly to take into account the mutual effects of absorption and diffraction. In particular, it can be shown[42] that partial suppression of absorption (Borrmann effect) will also occur in mosaic crystals in the diffraction region. However, in contrast to perfect crystals, the Borrmann effect is now relatively weak, and we shall not take it into account when we examine polarization phenomena in mosaic crystals, i.e., we shall assume that $\mathrm{Im}(\chi_{\mathbf{H}}\chi_{\bar{\mathbf{H}}}) = 0$.

The function $W(\Delta\Theta)$ is commonly regarded as a Gaussian or Lorentzian. The corresponding graphs of $W(\Delta\Theta)$ and $\tilde{W}(\Delta\Theta)$ are shown in Fig. 4. The very significant point is that $\tilde{W}(\Delta\Theta)$ decreases slowly with increasing $|\Delta\Theta|$: $\tilde{W}(\Delta\Theta) \approx -(\pi\Delta\Theta)^{-1}$, and, whatever the distribution of the mosaic blocks, the refractive index (1.26) reaches the universal form $\Delta n_\gamma \approx -C_\gamma^2\chi_{\mathbf{H}}\chi_{\bar{\mathbf{H}}}/(4\Delta\Theta \sin 2\Theta_B)$ for $|\Delta\Theta| \gg \Delta\Theta_b$. Hence, diffractive birefringence $\Delta n_\sigma - \Delta n_\pi$ is appreciable even outside the strong diffraction region. The quantity Δn_γ has an identical asymptotic behavior in perfect crystals (Sec. 1.3). The fact that, for large $|\Delta\Theta|$, the diffraction correction Δn_γ does not depend on the degree of perfection of the crystal can be understood qualitatively from the following considerations. For large $|\Delta\Theta|$, the significant point is that the crystal must be perfect over distances of the order of $L_b \gg \lambda|\Delta\Theta|$ since, for large distances, the phase difference between the diffracted waves is greater than π and, on average, the waves tend to cancel out one another. This means that, when the block size is $L_b \gg \lambda|\Delta\Theta|$, the radiation

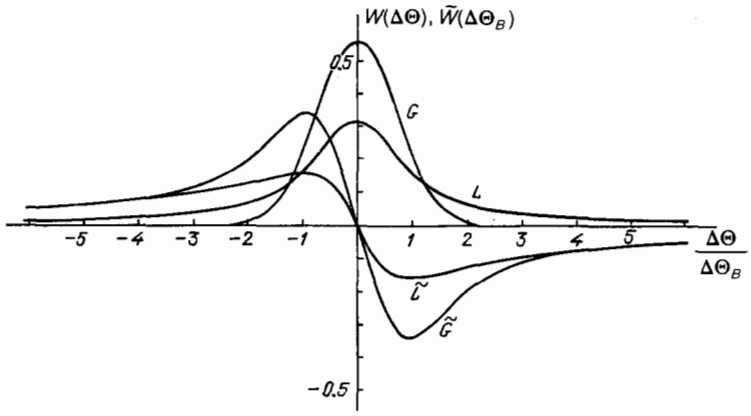

FIG. 4. Graphs of the functions $W(\Delta\Theta)$ and $\tilde{W}(\Delta\Theta)$ for the Gaussian (G and $\tilde{G}$) and Lorentzian (L and $\tilde{L}$) distributions (normalized so that $\int W_L(x)dx = \int W_G(x)dx$.

does not "feel" the imperfection of the crystal.

We now return to the examination of the terms in the transfer equations that describe the evolution of the polarization tensor of the direct beam. Since the refractive index is given by (1.26) for each of the polarization components, it can be shown[15,43] that terms describing the change in the polarization tensor of the direct beam by diffraction take the form $-QW(\Delta\Theta)\ (\hat{K}^2\hat{J}^0 + \hat{J}^0\hat{K}^2) + iQ\tilde{W}\ (\Delta\Theta)\ (\hat{K}^2\hat{J}^0 - \hat{J}^0\hat{K}^2)$. This finally leads us to the equation for $\partial\hat{J}^0/\partial s_0$ and the analogous equation for $\partial\hat{J}^{\mathbf{H}}/\partial s_{\mathbf{H}}$:

$$\frac{\partial\hat{J}^0}{\partial s_0} = -\mu\hat{J}^0 - QW(\Delta\Theta)(\hat{K}^2\hat{J}^0 + \hat{J}^0\hat{K}^2) + iQ\tilde{W}(\Delta\Theta)(\hat{K}^2\hat{J}^0 - \hat{J}^0\hat{K}^2) + QW(\Delta\Theta)\hat{K}\hat{J}^{\mathbf{H}}\hat{K}, \tag{1.28}$$

$$\frac{\partial\hat{J}^{\mathbf{H}}}{\partial s_{\mathbf{H}}} = -\mu\hat{J}^{\mathbf{H}} - QW(\Delta\Theta)(\hat{K}^2\hat{J}^{\mathbf{H}} + \hat{J}^{\mathbf{H}}\hat{K}^2) - iQ\tilde{W}(\Delta\Theta)(\hat{K}^2\hat{J}^{\mathbf{H}} - \hat{J}^{\mathbf{H}}\hat{K}^2) + QW(\Delta\Theta)\hat{K}\hat{J}^0K,$$

where $s_{\mathbf{H}}$ is the distance measured along the direction of propagation of the diffracted wave. The set of equations given by (1.28) provides a complete description of the polarization properties of diffraction in imperfect crystals with type I mosaic structure. It splits into four sets of equations for each of the elements of the tensors $\hat{J}^0$ and $\hat{J}_{\mathbf{H}}$. The equations for the diagonal elements are identical with the Darwin equations for the intensities of the σ and π polarized beams, and the only new feature is the presence of the equations for the off-diagonal elements. The solution of these equations for a crystal in the form of a plane-parallel plate presents no particular difficulty. A detailed analysis of the results has been given in Ref. 15, so that we shall confine our attention to a brief review of the basic results.

The main difference between the x-ray optics of imperfect and perfect crystals is that, even for a fixed angle $\Delta\Theta$, the diffracted beams become partially polarized whenever the polarization of the incident beam differs from the σ or π polarization. This polarization can be understood qualitatively from the following considerations. The incident-wave polarization varies as the radiation propagates through the crystal, so that waves diffracted at different depths have different polarizations and add inbcoherently, giving rise to a partially depolarized wave. An appreciable change in the polarization properties of diffracted beams occurs in mosaic crystals within the secondary extinction length $L_e^{II} = 2\pi\Delta\Theta_b/Q$. For type I mosaic structures $L_e^{II} \gg L_e^{I}$, but L_e^{II} can be comparable with the absorption length μ^{-1}, i.e., both $\mu L_e^{II} \gg 1$, and $\mu L_e^{II} \ll 1$. can occur. The effect of polarization is enhanced still further for quantities integrated over the diffraction region [the beam polarization tensors must be integrated as in the case of perfect crystals; see (1.15)].

Apart from polarization, diffraction birefringence of the diffracted and transmitted beams ensures that they become elliptically polarized (Fig. 5). For a linearly polarized incident beam, the elliptic polarization is right- or left-hand-

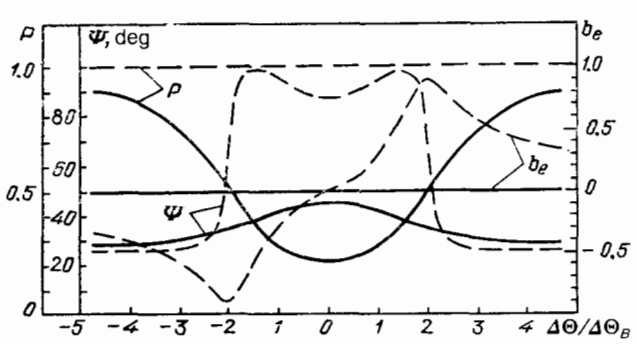

FIG. 5. Degree of polarization P, ratio of axes b_e, and rotation Ψ of the polarization elipse for a beam diffracted by a mosaic crystal as functions of the ratio $\Delta\Theta/\Delta\Theta_{\mathbf{B}}$; Laue geometry ($\Delta\Theta$—deviation from the Bragg conditions). Solid lines—symmetric Laue case $b = 1$, $\cos\Theta_B = \sqrt{3}/2$, dashed lines—asymmetric Laue case $b = 2$, $\cos\Theta_B = \sqrt{3}/2$. The incident beam was linearly polarized at 45° to the plane of scattering, $W(\Delta\Theta) = W_L(\varepsilon)$, crystal thickness $L = 2.5L_c^{II} = 5\pi\Delta\Theta_B/Q$.

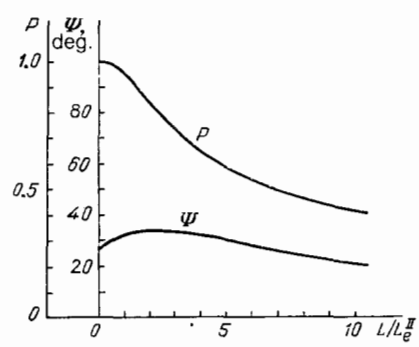

FIG. 6. Integral polarization parameters as functions of crystal thickness. Asymmetric Laue case ($b = 2$), linearly polarized incident beams with polarization at 45° to the vector σ (Ref. 15).

TABLE II. Polarization properties of diffracted wave for a polarized incident wave.

Properties	Crystals		
	kinematic	dynamic	mosaic
1. Different width of the diffraction regions for σ and π components	No	Yes	Yes
2. phase difference between σ and π components	No	Yes	Yes
3. depolarization (for a plane monochromatic wave)	No	No	Yes
4. depolarization integrated over the diffraction region	No	Yes	Yes

ed, depending on the sign of $\Delta\Theta$, and ellipticity practically disappears from the integrated parameters (if anomalous absorption can be neglected). Figures 5 and 6 show examples of differential and integral polarization parameters, and Table II compares the polarization parameters of perfect and imperfect crystals.

Experimental studies of the polarization properties of imperfect crystals are only just beginning, but they have already led to significant results. In addition to the early work,[10,12,44–46] we must particularly note the series of experimental studies by N. M. Olekhnovich *et al.*, who investigated the polarization properties of real crystals with different dislocation densities (see Ref. 14). They examined in detail the integrated[47–49] and differential[11,13,50,51] reflection coefficients for the σ and π polarizations, and have also observed diffractive birefringence and depolarization. Although, so far, experimental studies have been largely confined to σ and π polarizations, they have demonstrated that the Darwin theory of diffraction by mosaic crystals is frequently incapable of providing a quantitative description of the experimental data. For example, the ratio of the coefficients of reflection for σ and π polarized radiation (the so-called polarization coefficient[11,13,50,51]) reaches a plateau in the diffraction region (Fig. 7). This behavior can probably be explained by assuming that the dimensions of the individual blocks are so large that primary extinction becomes significant in each block.[50,51] However, some of the experimentally observed features have not received even a qualitative explanation. For example, it has been reported[53] that, for a certain dislocation density, the integrated reflection coefficient for π polarization is greater than that for σ polarization (Fig. 8).

In view of the foregoing, it is clear that further advances are necessary in the theory of diffraction by imperfect crystals, ands polarization measurements have to be brought in for the verification of theoretical predictions, since such measurements are the most informative. In particular, the Kato polarization theory[54] and its more developed versions[55,56] could be generalized to the case of arbitrary polarization.

The following general question has arisen: What is the maximum number of parameters that describe the polarization properties of each reflection (we have in mind quantities that can be measured with polarizers and analyzers without measuring the phases of the beams)? It is found that, since the σ and π polarizations do not mix in each Rayleigh scattering event, only four such parameters are necessary (each is a function of the angle of incidence and angle of reflection). These parameters can be, for example, the coefficients of reflection for σ and π polarizations and the complex coefficient of reflection for the off-diagonal components of the polarization tensor, i.e., the quantity relating the off-diagonal components of the polarization tensors of the incident and diffracted beams. We emphasize that the σ and π

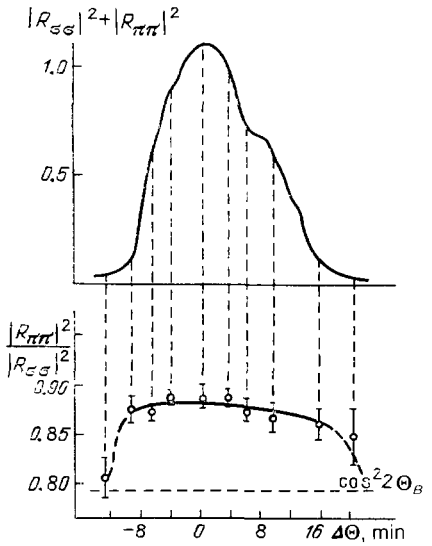

FIG. 7. Reflection coefficient $|R_{\sigma\sigma}|^2 + |R_{\pi\pi}|^2$ for unpolarized radiation and the ratio $|R_{\pi\pi}|^2/|R_{\sigma\sigma}|^2$ as functions of $\Delta\Theta$ for a dislocation density of 3×10^5 mm^{-2}. Symmetric Bragg case, Ge (III), CuK$_\alpha$ radiation.[50]

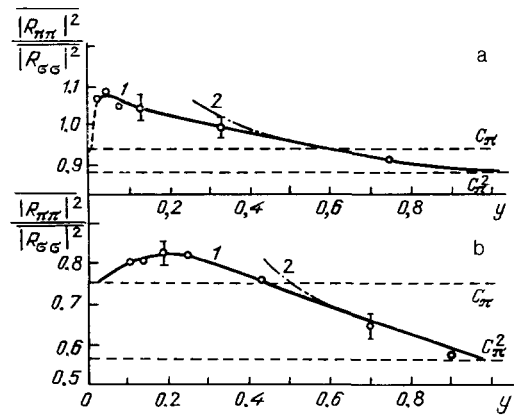

FIG. 8. Ratio of integral reflection coefficients for σ and π polarized beams as a functon of extinction factor y characterizing the degree of imperfection of the crystal; 200 (a) and 400 (b) reflections in LiF, CuK$_\alpha$ radiation.[53b] 1—experiment, 2—calculation including only primary extinction in individual mosaic blocks.

polarizations do not mix if diffraction is of the two-wave (or coplanar multiwave) type, and x-ray polarization anisotropy and rotation of the plane polarization are both absent.

It is important to note that measurements of the polarization properties of diffraction by perfect and, especially, imperfect crystals are also of metrological importance. Since crystals are used as monochromators, it is often important to know the quantitative polarization parameters of radiation after the monochromator (for example, in the case of structure analysis). The International Union of Crystallography[57] has therefore called for the investigation of the polarization properties of monochromators and methods for their determination[58–60]

2. Anisotropy of x-ray susceptibility. The traditional neglect of the anisotropy of x-ray susceptibility in discussions of diffraction by crystals (Sec. 1) is often fully justified.[61] However, this anisotropy is the reason for a number of qualitative effects, such as nondiffractive dichroism and birefringence (mostly near absorption edges), which are relatively obvious. A nontrivial qualitative consequence of this anisotropy is the appearance of reflections that are forbidden for symmetric reasons in the case of isotropic susceptibility, i.e., the appearance of "forbidden" reflections.[20–23]

Two complementary approaches can be naturally employed to investigate the anisotropy in x-ray susceptibility. The phenomenological approach is largely based on symmetry considerations, whereas the microscopic approach takes account of the specific atomic structure of the crystal. It is important to emphasize that symmetry restrictions on the x-ray susceptibility tensor can, in no way, be reduced to properties known in ordinary optics. Thus, when the symmetry properties of the susceptibility tensor in the optical range are investigated, the crystal is looked upon as a homogeneous medium.[62,63] Only the homogeneous part of the susceptibility $\hat{\chi}_0$, is then significant, and its symmetry is determined by the crystal point group, and is well known in optics.[62,63] In the case of x-ray diffraction, the inhomogeneous (periodic) part of $\hat{\chi}(r)$ becomes significant. Its symmetry is different at different points in the unit cell of the crystal and is determined by the point group of the crystal. The general properties of x-ray susceptibility are discussed in detail in Ref. 61, and the symmetry restrictions on $\hat{\chi}(r)$ are examined in Refs. 22 and 23 (see also the discussion below).

One of the manifestations of the anisotropy of susceptibility is the magnetic scattering of x-rays and magnetic dichroism, which occur in magnetically ordered crystals and are discussed in Sec. 2.4 below.

2.1. Birefringence and dichroism near absorption edges. A systematic description of the anisotropy of x-ray susceptibility can be constructed on the basis of the quantum-mechanical theory and requires a knowledge of the atomic and crystal electron wave functions (Refs. 26, 61, and 64). For our purposes, we need only be able to understand the physical reasons for anisotropy and to estimate its magnitude. We shall therefore slightly simplify the true picture of the interaction between x-rays and crystals. It is clear that the anisotropy of susceptibility appears as a consequence of the crystal structure, and is due to the distortion of the wave functions of free atoms by the crystal field. The anisotropy derives from the dispersion (resonance) correction to susceptibility, whereas the principal (potential) part of susceptibility is isotropic. The wave functions of the outermost electrons are the most highly distorted, but they provide a very small contribution to the dispersion corrections because the binding energy of the outer electrons is small in comparison with the energy of the x-ray photons. Appreciable dispersion corrections (of the order of the contribution of several electrons per atom) to the permittivity are provided by the innermost K and L shell electrons when the photon energy is close to the K or L absorption edges, although these shells are relatively undistorted by the crystal fields. In the simplest, dipole, approximation, the dispersion correction to the susceptibility of a crystal is given by[61,64]

$$\Delta\chi_{ik} = -\frac{r_e c^2}{m\omega^2}\sum_{j,m,s}\left[\frac{\langle 0|p_i^s|m\rangle\langle m|p_k^s|0\rangle}{E_0 - E_m + \hbar\omega - i(\Gamma_m/2)} + \frac{\langle 0|p_k^s|m\rangle\langle m|p_i^s|0\rangle}{E_0 - E_m - \hbar\omega}\right]_j \times \delta(\mathbf{r} - \mathbf{r}_j), \qquad (2.1)$$

where $\mathbf{p}^s - i\hbar\nabla^s$ is the momentum operator acting on the coordinate of the sth charge, $|0\rangle$ is the wave function of the initial state and of the final state that coincides with it (we are confining our attention to elastic processes), and $|m\rangle$ represents the wave functions of intermediate states that can lie either in the discrete or continuous spectrum. The origin of the anisotropy of susceptibility can be seen from (2.1): although the wave functions of the initial (and final) states are relatively undistorted, the wave functions of the intermediate states $|m\rangle$ can be greatly distorted, so that the product of the matrix elements $\langle 0|p_i|m\rangle\langle m|p_k|0\rangle$ does not reduce to the isotropic component. We note that, in the dipole approximation that we are considering here, the eigenpolarizations are found to be linear for the tensor (2.1). The real part of (2.1) is responsible for birefringence and the imaginary part for dichroism (there is no circular birefringence and dichroism). Moreover, the dispersion corrections are not very dependent on the transferred momentum (i.e., on the reflection $\mathbf{H}$). The last point is related to the fact that spatial dispersion effects are weak for the radii a_K and a_L of the K and L shells with energies in the x-ray range.

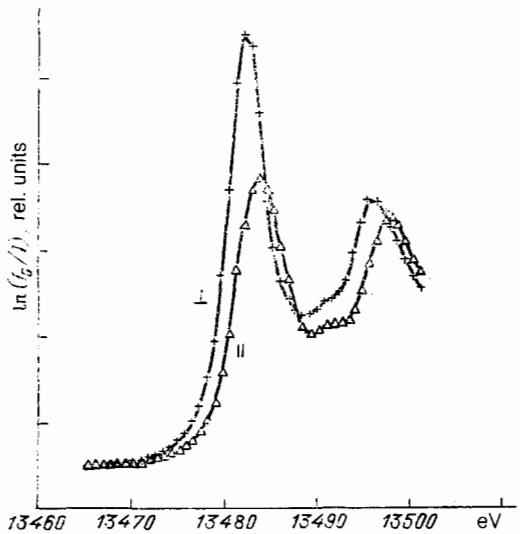

FIG. 9. X-ray absorption coefficients of $KBrO_3$ for radiation polarized parallel and perpendicular to the fourfold axis near K absorption edge of bromine.[20]

Numerous experimental[6,20,21,65,66] (see Fig. 9) and theoretical[26,61,64] investigations have shown that the dispersion corrections and the associated anisotropy of susceptibility reach their maxima in the immediate neighborhood (~ 10 eV) of the absorption edge (the so-called XANES, i.e., X-ray Absorption Near Edge Structure). Below the absorption edges, the main contribution to anisotropy is provided by bound excited states, whereas Bloch electron states in the crystal provide this contribution immediately above the edge.

Anisotropy decreases rapidly with increasing photon energy well above the absorption edge ($\gtrsim 100$ eV) in the EXAFS (Extended X-ray Absorption Fine Structure) region, but is still experimentally noticeable.[20,21] In this region, we can carry out a semiphenomenological evaluation of $\Delta\hat{\chi}$, for which, in intermediate states, we can take into account the diffraction of photoelectrons by atoms surrounding a given atom (it is well known that photoelectrons are preferentially emitted in the direction of the polarization vector of the incident x-ray photon). This diffraction is very dependent on the distance to the nearest-neighbor atoms and on the form factors of these atoms. The result of all this is that the anisotropy of the environment of a given atom has an appreciable effect on the anisotropy of $\Delta\hat{\chi}$ in the EXAFS region. Thus, although the physical reason for the onset of the anisotropy of susceptibility near x-ray absorption edges is relatively obvious, a quantitative evaluation is relatively complicated.[61,64] It is therefore natural to perform a symmetry analysis of the susceptibility tensor, which does not involve a detailed consideration of a model.

2.2. Symmetry restrictions on the x-ray susceptibility tensor of a crystal. The x-ray susceptibility of a nonmagnetic crystal is described by the symmetric tensor of rank two $\chi_{ik}(\mathbf{r}) = \chi_{ki}(\mathbf{r})$, which is unaffected by transformations belonging to the space group of the crystal. The easiest way of finding the general form of this tensor is as follows. The atoms in a crystal structure occupy a certain definite regular set of points (one or more). It is therefore sufficient (1) to determine the tensor $\hat{\chi}^b(\mathbf{r})$ for a single basis atom in a given lattice, taking into account the point symmetry of the atomic site, (2) to obtain the tensor $\hat{\chi}^j(\mathbf{r})$, found for the jth atom in the regular set of points, by transforming the tensor $\hat{\chi}^b(\mathbf{r})$ by a symmetry operation relating the positions of the basis and jth atoms in the crystal, and (3) to obtain the total tensor $\hat{\chi}(\mathbf{r})$ as the sum over all atoms in the given regular structure and over all the regular sets of points occupied by atoms in the given crystal.

To find the general form of $\hat{\chi}(\mathbf{r})$, we must therefore know how the tensor $\hat{\chi}(\mathbf{r})$ transforms under the symmetry operations. Suppose that the tensor $\hat{\chi}(\mathbf{r})$ is given in space. If we apply to it a transformation g that includes the point transformation (rotation or reflection) and translation, the tensor $\hat{\chi}_g(\mathbf{r})$, obtained as a result of this, is related to the original tensor $\hat{\chi}(\mathbf{r})$ as follows (see, for example, Refs. 67 and 68):

$$\hat{\chi}_g(\mathbf{r}) = \hat{R}_g\hat{\chi}(\mathbf{r}_g)\hat{R}_g^{-1}, \tag{2.2}$$

where $\mathbf{r}_g = \hat{R}_g^{-1}(\mathbf{r} - \mathbf{a}_g)$, $\hat{R}_g$ is the point transformation matrix and $\mathbf{a}_g$ is the translation vector. If the tensor $\hat{\chi}(\mathbf{r})$ is invariant under g, then $\hat{\chi}_g(\mathbf{r}) = \hat{\chi}(\mathbf{r})$.

If the basis atom lies at a point whose symmetry is described by the point group g, the susceptibility tensor $\hat{\chi}^b(\mathbf{r})$ of this atom will obviously be invariant under any transformation g in this group, i.e., in this case $\hat{\chi}^b(\mathbf{r})$ must satisfy the following relation that ensues from (2.2):

$$\hat{\chi}^b(\mathbf{r}) = \hat{R}_g\hat{\chi}^b(\hat{R}_g^{-1}\mathbf{r})\hat{R}_g^{-1}. \tag{2.3}$$

The tensor satisfying this relation can be obtained by averaging an arbitrary symmetry tensor $\hat{\alpha}(\mathbf{r})$ over the group G (Ref. 68):

$$\hat{\chi}^b(\mathbf{r}) = \langle\hat{\alpha}(\mathbf{r})\rangle_G \equiv \sum_{g\in G}\hat{R}_g\hat{\alpha}(\hat{R}_g^{-1}\mathbf{r})\hat{R}_g^{-1}. \tag{2.4}$$

Having determined in this way the most general form of $\hat{\chi}^b(\mathbf{r})$ for the basis atom, we can now use (2.2) to find the tensors $\hat{\chi}^j(\mathbf{r})$ for the remaining atoms in the given lattice, taking g to be the symmetry operation g_j relating the position of the jth atom to the basis atom. Of course, all these operations can be performed for any regular set of points occupied by atoms in a given crystal.

All this finally yields the most general form of the tensor $\hat{\chi}(\mathbf{r})$ that is consistent with the space symmetry group of the crystal. This automatically takes into account the difference between the electron density of the atom and the spherically symmetric density (the electron density is a scalar proportional to the trace of the tensor $\hat{\chi}(\mathbf{r})$).

In its symmetry properties, the tensor $\hat{\chi}(\mathbf{r})$ differs radically from the susceptibility tensor in the optical range. In particular, $\hat{\chi}(\mathbf{r})$ does not reduce to a scalar even in cubic crystals. The local symmetry of $\hat{\chi}(\mathbf{r})$ is different at different points of the unit cell. We note that the general form of $\hat{\chi}(\mathbf{r})$ can be found even without resorting to the particular atomic structures of a crystal,[22] but the approach employed above is clearer and enables us to identify the contributions to $\hat{\chi}(\mathbf{r})$ due to different species of atoms.

If, in addition to the symmetry properties, we take into account the physical origin of the anisotropy, we can find further restrictions on $\hat{\chi}(\mathbf{r})$. Thus, since the radii of the K and L shells are small, we can substitute $\mathbf{r} = 0$ in the dispersive part of $\hat{\chi}^b(\mathbf{r})$ in (2.3) and (2.4), which substantially simplifies all the calculations and, for certain special dispositions of the atoms, may modify the form of the tensor $\hat{\chi}(\mathbf{r})$ (examples are given below).

To find the intensity and the polarization properties of individual reflections, it is convenient to introduce the tensor form of the structure amplitude $\hat{F}^{\mathbf{H}}$, which is proportional to the Fourier component of the susceptibility $\hat{\chi}^{\mathbf{H}}$:

$$\hat{F}^{\mathbf{H}} = -\frac{\pi V}{r_e\lambda^2}\hat{\chi}^{\mathbf{H}} \equiv -\frac{\pi}{r_e\lambda^2}\int\hat{\chi}(\mathbf{r})\exp(-i\mathbf{H}\mathbf{r})\,d\mathbf{r}, \tag{2.5}$$

where all the symbols have the same meaning as in (1.2). The amplitude $\hat{F}^{\mathbf{H}}$ is usefully divided into the isotropic and intrinsically anisotropic parts:

$$\hat{F}^{\mathbf{H}} = F_{\mathbf{H}}\hat{I} + \Delta\hat{F}^{\mathbf{H}}, \tag{2.6}$$

where $\mathbf{F}_{\mathbf{H}}$ is the usual structure amplitude, $\hat{I}$ is the unit matrix, and the anisotropic part is defined so that $Sp(\Delta\hat{F}^{\mathbf{H}}) = 0$.

The symmetry restrictions on $\hat{\chi}(\mathbf{r})$ influence the tensor form of $\hat{F}^{\mathbf{H}}$ (Refs. 22 and 23). For an arbitrary vector $\mathbf{H}$, there are no restrictions on the form of $\Delta\hat{F}^{\mathbf{H}}$ and, just like any other traceless symmetric tensor, $\Delta\hat{F}^{\mathbf{H}}$ has five indepen-

dent complex components. However, if the vector **H** points along the symmetry axes, the number of independent components of the tensor $\Delta\hat{F}^{\mathbf{H}}$ is reduced (we take the z-axis to lie along **H**): if **H** is parallel to axis 2, $\Delta F^{\mathbf{H}}_{xz} = \Delta F^{\mathbf{H}}_{yz} = 0$; if **H** is parallel to axes 3, 4, 6, $\Delta F^{\mathbf{H}}_{xy} = \Delta F^{\mathbf{H}}_{xz} = \Delta F^{\mathbf{H}}_{yz} = 0$ and $\Delta F^{\mathbf{H}}_{xx} = \Delta F^{\mathbf{H}}_{yy} = -1/2\Delta F^{\mathbf{H}}_{zz}$. If **H** is parallel to the mirror reflection plane, then, by choosing the x-axis to be perpendicular to this plane, we have $\Delta F^{\mathbf{H}}_{xy} = \Delta F^{\mathbf{H}}_{xz} = 0$.

The intensity and polarization properties of reflections with the tensor amplitude (2.6) can be found in both the kinematic and two-wave dynamic approximations by analogy with the analysis of diffraction of Mössbauer radiation[69] and the diffraction of light by liquid crystals.[70] In most cases, $\Delta\hat{F}^{\mathbf{H}}$ is small in comparison with $F_{\mathbf{H}}$, and the entire analysis can be based on perturbation theory. The most interesting cases are those for which $F_{\mathbf{H}} = 0$ by symmetry considerations ("forbidden" reflections) and $\Delta\hat{F}^{\mathbf{H}} \neq 0$, i.e., the inclusion of anisotropy reduces the suppression of reflection (see next section).

2.3. Forbidden reflections. It is well known that the systematic suppression of reflections is observed in x-ray diffraction by crystals, i.e., the structure amplitudes of some of the reflections vanish systematically because the atoms in the interior of the unit cell are found to be in a number of symmetrically related positions.[32] The set of these forbidden reflections is determined by the space group of the crystal, and is given in Ref. 71. However, the standard conditions given in Ref. 71 were obtained on the assumption that the atomic scattering factors were identical for all atoms in equivalent positions, i.e., it was actually assumed that the atoms forming the crystal were spherically symmetric. In reality, the atoms in the crystal are not spherically symmetric because of interactions between them, which means that they are not equivalent from the point of view of scattering, and this can give rise to the appearance of the "forbidden" reflections. More precisely, it may be said that atoms lying in equivalent crystallographic positions may be nonequivalent from the point of view of their interaction with electromagnetic (x-ray) radiation, and the scattering amplitudes for such atoms may be different.

There are several physical factors that produce this difference between the scattering amplitudes corresponding to crystallographically equivalent atoms. The best known are the nonspherical electron density distribution of the atom, and the anisotropy and anharmonicity of thermal vibrations of atoms[72–74] (the 222 type reflections in crystals with diamond structure constitute a well-known example of this). Another example is provided by the dependence of the scattering amplitude on the electron spin, which leads to very weak magnetic reflections when x-rays are diffracted by magnetically-ordered crystals (Sec. 2.4). The anisotropy of x-ray susceptibility can also lead to a difference between the scattering amplitudes, since crystallographically equivalent atoms can be related by a symmetry operation containing rotation, and under rotations, the anisotropy tensor can alter the orientation of its principal axes.

It is well known that the conditions for possible Bragg reflections by a crystal with a given space group can be different for general and particular positions of atoms in the unit cell.[32,71] If we take into account the nonspherical nature of the atomic electron density and the thermal motion of atoms, the conditions for special positions are violated, but those imposed on the general positions are not. However, the latter may also be violated if we take into account the anisotropy of susceptibility. Clearly, the conditions associated with the centering of lattices remain valid even in this case, since the transformation properties of tensors and scalars are the same under pure translations. However, the restrictions on reflections that are due to the presence of slip planes or helical axes are no longer valid (Refs. 20–24), and we shall prove this rigorously. However, let us first give a clear interpretation of this phenomenon.

Suppose the crystal has a slip plane (Fig. 10a), i.e., for example, the structure is invariant under reflections in the yz plane and displacements along the z axis. Atoms in positions A and B are crystallographically equivalent, but the corresponding susceptibility tensors (indicated symbolically by the ellipses) are rotated relative to one another, and these atoms are polarized differently by the incident x-ray waves. In the case of the $00l$ reflections with $l = 2n + 1$, these atoms scatter in antiphase. If we ignore the anisotropy of susceptibility, waves scattered by these atoms will extinguish one another, and the reflections will be forbidden. When the anisotropy is taken into account, scattering by atoms A and B will be different in both intensity and polarization, and this will mean that the suppression of the reflections will not occur. A similar mechanism can lead to the removal of the suppression of reflections that are "forbidden" by helical axes (Figs. 10b and c).

We now turn to a detailed symmetry analysis. A crystal transforms into itself under all symmetry transformations belonging to its space group. Consequently, the structure amplitudes $\hat{\mathbf{F}}^{\mathbf{H}}$ must remain unaltered. In the case of the slip-plane reflection examined above, a displacement by half

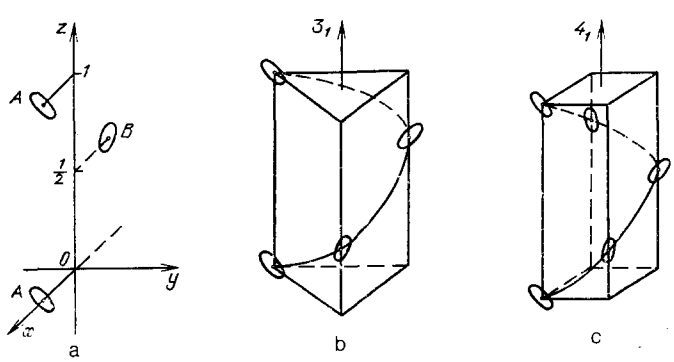

FIG. 10. Effect of symmetry elements on atoms with anisotropic susceptibility: a—slip plane c, b—3_1 axis, c—4_1 axis.

the period along the z axis leads to the multiplication of the structure amplitude of the $0kl$ reflection by $\exp(i\pi l) = (-1)^l$. Reflection by the yz plane (i.e., $x \to -x$) leads to a change in the sign of the xy and xz components of the tensor structure amplitude. Since the structure amplitude must be invariant under this transformation, we find that the xy and xz components must be annulled in the structure amplitude for $l = 2n$ (allowed reflections), whereas for $l = 2n + 1$ ("forbidden" reflections), all the components other than the xy and xz components are annulled. It is thus clear that symmetry does not demand the complete annulment of the structure amplitudes of reflections with $l = 2n + 1$, and the suppression of these reflections is removed, but only when the susceptibility is anisotropic.

Reflections that are "forbidden" by the presence of helical axes can be examined similarly. Suppose that the helical axis N_j points along the z axis, i.e., the crystal is invariant under the combined operations of rotation by the angle $\varphi = 2\pi/N$ about the z axis and displacement along the z axis by the fraction j/N of the period ($N = 2,3,4,6$; $j = 1,...,N-1$). The tensor structure amplitude $\hat{F}^{00l}$ transforms into $R_\varphi F^{00l} \hat{R}_\varphi^{-1}$ under rotation, and acquires the further factor $\exp(2\pi ilj/N)$ under displacement. Consequently, the invariance of $\hat{F}^{00l}$ under this operation requires that the condition

$$\hat{F}^{00l} = \hat{R}_\varphi \hat{F}^{00l} \hat{R}_\varphi^{-1} \exp(2\pi ilj N^{-1}), \tag{2.7}$$

must be satisfied, where the rotation matrix $\hat{R}_\varphi$ has the form

$$\hat{R}_\varphi = \begin{pmatrix} \cos\varphi & \sin\varphi & 0 \\ -\sin\varphi & \cos\varphi & 0 \\ 0 & 0 & 1 \end{pmatrix}. \tag{2.8}$$

If there is no anisotropy, it follows from (2.7) that $\hat{F}^{00l} = 0$ for $l \neq Nn/j$, where n is an arbitrary integer, i.e., all these reflections are forbidden.[71] When the anisotropy is taken into account, it follows from (2.7) that the suppression of these reflections is removed, save for some rare exceptions (Table III). It is clear from Table III that, for each "forbidden" reflection, all the components of the tensor $\hat{F}^{\mathbf{H}}$ are expressed in terms of, at most, two independent parameters, say, F_1 and F_2, which may be complex. To avoid misunderstanding, we emphasize that these parameters are different for different reflections and, in general, they depend on the wavelength. Their numerical values can be calculated from microscopic theory. The phenomenological theory that we are discussing shows only that these parameters need not be zero if the crystal has only a helical axis or only a reflecting slip plane. Other symmetry elements can lead to additional relationships between F_1 and F_2 and, in particular, may reduce them (or one of them) to zero. For example, reflections with $|h| = |k| = |l|$ continue to be forbidden in cubic crystals.[23] Moreover, these parameters are annuled because atoms that contribute to anisotropy lie in positions of relatively high symmetry.

It follows from Table III that the tensor $\hat{F}^{\mathbf{H}}$ can have a different form for different types of reflection, and it may be expected that the properties of these types of reflection are also different (see below). It is interesting to note that some of the reflections associated with helical axes remain forbidden. For example, in the case of the 6_3 axis, the necessary presence of axis 3 leads to the absence of anisotropy in the xy plane, so that the suppression of reflections with $l = 2n + 1$ is not removed, and $\hat{F}^{00l} = 0$ for them. For axes 6_1 and 6_5, reflections with $l = 6n + 3$ are also found to remain forbidden. When the quadrupole interaction is taken into account, these reflections may become allowed, and this can be used to detect the quadrupole mechanism of interaction between x-rays and crystal atoms.

The intensity and, especially, the polarization properties of reflections are altered when anisotropy is taken into account. For allowed reflections, these changes take the form of corrections (the exception is provided by the possibility of 90° scattering of π-polarized waves) and can be found in both the kinematic and dynamic theories. The polarization properties become radically different for forbidden reflections, and are found to be very unusual. For example, a σ-polarized incident wave can produce a π-polarized diffraction wave, and vice versa. Since the structure amplitudes of these reflections are relatively small, we can use the kinematic approximation for them. The amplitude of the dif-

TABLE III. Components of the tensor structure amplitude $\hat{F}^{\mathbf{H}}$ and the index l for "forbidden" reflections (the other components are $F^{\mathbf{H}}_{yy} = -F^{\mathbf{H}}_{xx}, F^{\mathbf{H}}_{zz} = 0$, $F^{\mathbf{H}}_{yx} = F^{\mathbf{H}}_{xy}$, $F^{\mathbf{H}}_{zy} = F^{\mathbf{H}}_{yz}$, $F^{\mathbf{H}}_{zx} = F^{\mathbf{H}}_{xz}$), $n = 0, \pm 1, \pm 2...$.

Hel. axis or slip plane	$F^{\mathbf{H}}_{xx}$	$F^{\mathbf{H}}_{xy}$	$F^{\mathbf{H}}_{xz}$	$F^{\mathbf{H}}_{yz}$	l	Type of reflection
2_1	0	0	F_1	F_2	$2n+1$	I
3_1	F_2	$\pm iF_2$	F_1	$\mp iF_1$	$3n\pm1$	II
3_2	F_2	$\mp iF_2$	F_1	$\pm iF_1$	$3n\pm1$	II
4_1	0	0	F_1	$\mp iF_1$	$4n\pm1$	I
4_1	F_1	F_2	0	0	$4n+2$	II
4_2	F_1	F_2	0	0	$2n+1$	II
4_3	0	0	F_1	$\pm iF_1$	$4n+1$	I
4_3	F_1	F_2	0	0	$4n+2$	II
6_1	0	0	F_1	$\mp iF_1$	$6n+1$	I
6_1	F_1	$\mp iF_1$	0	0	$6n\pm2$	II
6_1	0	0	0	0	$6n+3$	
6_2	F_1	$\mp iF_1$	0	0	$3n\pm1$	II
6_3	0	0	0	0	$2n+1$	
6_4	F_1	$\pm iF_1$	0	0	$3n+1$	II
6_5	0	0	F_1	$\pm iF_1$	$6n\pm1$	I
6_5	F_1	$\pm iF_1$	0	0	$6n\pm2$	II
6_5	0	0	0	0	$6n+3$	
c	0	F_1	F_2	0	$2n+1$	II

fracted wave is then given by

$$\mathbf{E}^{\mathrm{d}} = A\hat{F}^{\mathbf{H}}\mathbf{E}^{i}, \tag{2.9}$$

where the factor A is the same as in (1.3). This expression enables us to evaluate the intensity and polarization of the diffracted wave for any polarization of the incident wave. This can be conveniently carried out in terms of the quantity $I_{\alpha\beta}$, which describes the intensity of the component with arbitrary (β) polarization in the reflected beam for arbitrary (α) polarization of the incident beam:

$$I_{\alpha\beta} = |A|^2 |\boldsymbol{\beta}^* \hat{F}^{\mathbf{H}} \boldsymbol{\alpha}|^2, \tag{2.10}$$

where α and β are the corresponding polarization vectors. The polarization of the diffracted wave is determined by the unit vector $\beta^d = \mathbf{E}^d/|\mathbf{E}^d|$. We note that the vector (β^d) may or may not depend on the polarization vector of the incident beam (see below).

If the incident radiation is σ- or π-polarized or unpolarized, the intensity of the reflection is determined, respectively, by the following expressions:

$$I_\sigma = I_{\sigma\sigma} + I_{\sigma\pi}, \tag{2.11}$$

$$I_\pi = I_{\pi\sigma} + I_{\pi\pi}, \tag{2.12}$$

$$I_{\mathbf{H}} = \frac{1}{2}(I_\sigma + I_\pi), \tag{2.13}$$

where

$$\begin{aligned} I_{\sigma\sigma} &= |A|^2 |\boldsymbol{\sigma}\hat{F}^{\mathbf{H}}\boldsymbol{\sigma}|^2, \\ I_{\pi\pi} &= |A|^2 |\boldsymbol{\pi}_{\mathbf{H}}\hat{F}^{\mathbf{H}}\boldsymbol{\pi}_0|^2, \\ I_{\sigma\pi} &= I_{\pi\sigma} = |A|^2 |\boldsymbol{\pi}_{\mathbf{H}}\hat{F}^{\mathbf{H}}\boldsymbol{\sigma}|^2 = |A|^2 |\boldsymbol{\sigma}\hat{F}^{\mathbf{H}}\boldsymbol{\pi}_0|^2. \end{aligned} \tag{2.14}$$

Let us examine, for example, the properties of forbidden reflections associated with the presence of helical axes. It is clear from Table III that all these reflections can be divided into two basic types, namely, reflections for which $F^{\mathbf{H}}_{xx}, F^{\mathbf{H}}_{yy}$, and $F^{\mathbf{H}}_{xy}$ are all zero (type I) and all the other reflections (type II). We shall show that the polarization properties of these two types of reflection are significantly different.

Type I reflections have the simplest polarization properties. It follows directly from (2.9)–(2.14) and from Table III that $I_{\sigma\sigma} = I_{\pi\pi} = 0$ and $I_{\mathbf{H}} = I_\sigma = I_\pi = I_{\sigma\pi} = I_{\pi\sigma}$ for all type I reflections, where for axis 2_1 the intensity is given by

$$I_{\sigma\pi} = |A|^2 \cos^2\Theta_{\mathrm{B}} \{|F_1|^2 \sin^2\varphi_{\mathbf{H}} + |F_2|^2 \cos^2\varphi_{\mathbf{H}} - \mathrm{Re}\,(F_1 F_2^*) \sin 2\varphi_{\mathbf{H}}\}, \tag{2.15}$$

in which $\varphi_{\mathbf{H}}$ is the azimuthal angle of rotation around the vector $\mathbf{H}$ (z axis), measured from the x axis, whereas for axes 4_1, 4_3, 6_1, 6_5, the intensity has the simpler form

$$I_{\sigma\pi} = |A|^2 \cos^2\Theta_{\mathrm{B}} |F_1|^2. \tag{2.16}$$

A σ-polarized incident wave will therefore produce a π-polarized diffracted wave for type I reflections, and vice versa. An unpolarized beam will produce an unpolarized diffracted beam. Type I reflections disappear in the case of backward angle diffraction (since $\cos\Theta_B = 0$). In the case of the 4_1, 4_3, 6_1, 6_5 axes, the intensity of these reflections does not depend on the azimuthal angle $\varphi_{\mathbf{H}}$.

The intensity of type II reflections is given by the following expressions that ensue from (2.9)–(2.14) and Table III;

for axes 3_1 and 3_3

$$\begin{aligned} I_\sigma &= |A|^2 \{|F_1|^2 \cos^2\Theta_{\mathrm{B}} + |F_2|^2 (1 + \sin^2\Theta_{\mathrm{B}}) \\ &\quad + \sin 2\Theta_{\mathrm{B}} [\mathrm{Re}\,(F_1 F_2^*) \cos 3\varphi_{\mathbf{H}} \mp \mathrm{Im}\,(F_1 F_2^*) \sin 3\varphi_{\mathbf{H}}]\}, \\ I_\pi &= I_\sigma - |A|^2 |F_2|^2 \cos^2\Theta_{\mathrm{B}} (1 + \sin^2\Theta_{\mathrm{B}}) \end{aligned} \tag{2.17}$$

for axes 4_1, 4_2, 4_3

$$\begin{aligned} I_\sigma &= |A|^2 [|F_1|^2 B(\varphi_{\mathbf{H}}) + |F_2|^2 C(\varphi_{\mathbf{H}}) \\ &\quad + \mathrm{Re}\,(F_1 F_2^*) \cos^2\Theta_{\mathrm{B}} \sin 4\varphi_{\mathbf{H}}], \\ I_\pi &= |A|^2 \sin^2\Theta_{\mathrm{B}} [|F_1|^2 C(\varphi_{\mathbf{H}}) + |F_2|^2 B(\varphi_{\mathbf{H}}) \\ &\quad - \mathrm{Re}\,(F_1 F_2^*) \cos^2\Theta_{\mathrm{B}} \sin 4\varphi_{\mathbf{H}}], \\ B(\varphi_{\mathbf{H}}) &= 1 - \cos^2\Theta_{\mathrm{B}} \sin^2 2\varphi_{\mathbf{H}}, \\ C(\varphi_{\mathbf{H}}) &= 1 - \cos^2\Theta_{\mathrm{B}} \cos^2 2\varphi_{\mathbf{H}}; \end{aligned} \tag{2.18}$$

for axes 6_1, 6_2, 6_4, and 6_5

$$\begin{aligned} I_\sigma &= |A|^2 |F_1|^2 (1 + \sin^2\Theta_{\mathrm{B}}), \\ I_\pi &= I_\sigma \sin^2\Theta_{\mathrm{B}} \end{aligned} \tag{2.19}$$

where the upper and lower signs in (2.17) correspond to the two possibilities $F^{\mathbf{H}}_{xy} = \pm iF^{\mathbf{H}}_{xx}$ (see Table III). In contrast to type I reflections, the type II intensities are different for σ- and π-polarized beams. It is clear from (2.18) and (2.19) that, for small Bragg angles, the σ-polarized beams have a higher intensity. For three- and sixfold helical axes, the type II reflections have chiral properties, i.e., their intensity is different for right- and left-handed circular polarizations of the incident beam. For example, for backward Bragg reflections ($\Theta_B = 90°$), (2.9) shows that only a component with a definite circular polarization (right if $F^{\mathbf{H}}_{xy} = -iF^{\mathbf{H}}_{xx}$, and left if $F^{\mathbf{H}}_{xy} = iF^{\mathbf{H}}_{xx}$) will undergo diffractive reflection (the diffracted beam having the same circular polarization). The wave with the opposite circular polarization will not be diffracted. It follows that, for $\Theta_B = 90°$, the crystal works as a circular polarizer and, for any polarization of the incident beam, the diffracted beam has a particular circular polarization that depends on l and on whether or not the helical axis is right- or left-handed (Table III). When $\Theta_B < 90°$, the polarization of these type II reflections are elliptic rather than circular. For sixfold axes, the ratio of the axes of the polarization ellipse is $\sin\Theta_B$, where the major axis is parallel to the vector σ and the sign of the polarization (right- or left-handed) is determined as for $\Theta_B = 90°$. For threefold helical axes, the ratio of the axes of the polarization ellipse is a complicated function of Θ_B, and we shall not reproduce here the relationship between the parameters F_1 and F_2. For fourfold helical axes, we have chiral type II reflections if $\mathrm{Im}(F_1 F_2^*) \neq 0$.

We particularly note that the intensity of the "forbidden" reflections depends on the azimuthal angle (even for an unpolarized incident beam). By studying this dependence, we can determine the magnitude of the components of $\hat{F}^{\mathbf{H}}$ (the parameters F_1 and F_2) and their relative phase. It has been shown[23] that the azimuthal dependence can also be used to determine selectively the coordinates of atoms contributing to the anisotropy.

Let us illustrate all this by considering the example of

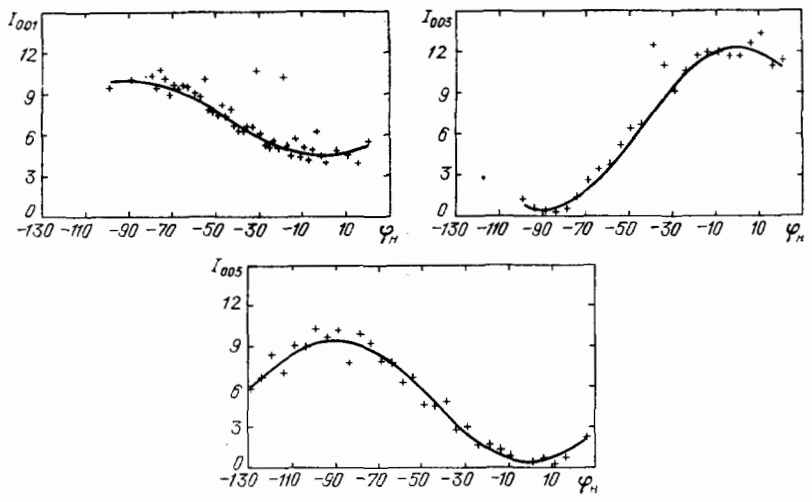

FIG. 11. Observed (points) and calculated (curves) azimuthal dependence of the intensity of "forbidden" reflections $NaBrO_3$ (Ref. 21); 13474-eV unpolarized radiation (below the K edge of bromine). The points that depart substantially from the theoretical curve correspond to the Renninger reflections.

$00l$ ($l = 2n + 1$) reflections in a crystal with space group $P2_13$ and four atoms in special positions (a) with point symmetry 3 and coordinates x,x,x; $1/2 + x$, $1/2 - x,\bar{x}$; $1/2 - x,\bar{x},1/2 + x;\bar{x},1/2 + x,1/2 - x$. The anisotropy of susceptibility of atoms in positions of this symmetry is characterized by the susceptibility difference $\chi_\parallel - \chi_\perp$ (parallel and perpendicular to axis 3). Consequently, both F_1 and F_2 can be expressed in terms of this difference and the coordinate x. It can be shown that $F_1/F_2 = i\,tg(2\pi/x)$ and that the intensity of the $00l(l = 2n + 1)$ reflections is proportional to $1 - \cos 4\pi lx \cos 2\varphi_{\mathbf{H}}$. The azimuthal dependence of the intensity of "forbidden" reflections can therefore be used to determine the coordinate x. This was recently demonstrated[21] (Fig. 11) for $NaBrO_3$ crystals.

"Forbidden" reflections can also be used in other ways. They are useful in the interpretation of spectra near absorption edges (in contrast to absorption coefficients, these reflections provide information on not only the imaginary, but also the real part of the atomic factors, which is moreover not averaged over the unit cell). They can be used to determine the phases of some of the reflections[75] and, together with polarization measurements, they can be used to establish the absolute configuration of enantiomers. In cubic crystals, these reflections afford probably the only way of observing the anisotropy of the susceptibility of individual atoms.

The so-called Renniger reflections, i.e., the indirect excitation of "forbidden" reflections via allowed reflections,[72,76] can impede the observation of the "forbidden" reflections. However, this type of multiwave diffraction is possible only for certain particular azimuthal angles $\varphi_{\mathbf{H}}$, which are readily calculated (the indirect excitations are actually responsible for the individual departures of the points from the curves of Fig. 11). Moreover, interference with the Renniger reflections can be used to determine the phase of the tensor structure amplitude of "forbidden" reflections (for the scalar case, this method of solving the "phase problem" has already been used in Refs. 77–79).

2.4. Magnetic scattering. The principal contribution to the scattering of x-rays is due to the Thomson mechanism whereby x-rays are scattered by the charge of the electron. Classically, this can be looked upon as the dipole emission by a charge accelerated in the electric field of the x-ray wave. However, in addition to its charge the electron also has an intrinsic magnetic moment $-2\mu_B\mathbf{s}$ and a magnetic moment due to its orbital motion in the atom, $-\mu_B\mathbf{l}$. The interaction of the x-ray wave with these moments leads to magnetic scattering that is sensitive to the magnetic structure of the medium. In classical language, the principal channels of this magnetic scattering can be described as follows[25,80] (Fig. 12): (1) magnetic quadrupole emission by the magnetic moment $\boldsymbol{\mu}$ moving under the influence of the force $-e\mathbf{E}$, (2) electric dipole emission of a charge accelerated by the force $-\nabla(\boldsymbol{\mu}\mathbf{H})$, and (3) magnetic dipole emission by the magnetic moment due to rotation under the influence of the couple $[\boldsymbol{\mu}\mathbf{H}]$. Moreover, magnetic scattering can exhibit resonance phenomena,[81] e.g., the so-called resonance magnetic scattering that occurs via atomic energy levels split by the exchange interaction (the analog of Zeeman splitting).

It is clear from the foregoing that the polarization properties of magnetic scattering of x-rays are very different from those of Rayleigh scattering. Phenomenologically the presence of magnetic scattering corresponds to extra terms of the form $ie_{jkn}s_n$ in the susceptibility (e_{jkn} is a perfectly antisymmetric unit tensor) and to extra terms that depend explicitly on the wave vectors of the incident and scattered waves (equivalent to taking into account spatial dispersion). These terms lead, in particular, to different scattering of right- and left-polarized waves and to the rotation of the plane of polarization (Faraday effect).

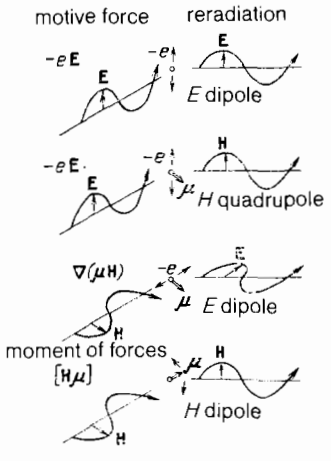

FIG. 12. Magnetic scattering of a photon by an atom in classical electrodynamics.[25]

The absolute magnitude of the magnetic scattering amplitude per electron is smaller by the factor $\hbar\omega/(mc^2)$ than the Rayleigh scattering amplitude, and some of the terms are smaller by the factor p/mc, where p is the typical electron momentum in the atom. In the x-ray region, both estimates yield a figure of approximately 0.01. Since, in the atom, only a small number of electrons have an uncompensated magnetic moment, and the formfactor of these electrons decreases rapidly with increasing angle of scattering, we find that the magnetic scattering amplitude is smaller than the Rayleigh amplitude of an atom by three or four orders of magnitude. Despite the fact that magnetic scattering is weak, the availability of synchrotron sources ensures that this can be a working method for the investigation of the magnetic properties of solids.

The quantum-mechanical approach is, of course, essential for the quantitative description of magnetic scattering. Although the corresponding formulas, in which the photon scattering cross section is a function of the electron spin, has been known for a relatively long time (for both free and bound electrons,[33,80,82] the suggestion that they could be used to investigate the magnetic properties of solids did not appear until 1970; see Ref. 24). The spin of the free electron ensures that the scattering cross section (Compton effect) is different, depending on whether the circular polarizations are parallel (+) or antiparallel (−) to the spin direction:[33]

$$\frac{d\sigma^{\pm}}{d\sigma} = \frac{r_e^2}{2}\left[1 + \cos^2\theta \pm \frac{2\hbar\omega}{mc^2}\cos\theta(\cos\theta - 1)\right], \quad (2.20)$$

where θ the scattering angle [formula (2.20) was obtained in the nonrelativistic approximation in which $\hbar\omega \ll mc^2$]. The first experiments on the Compton scattering of polarized x-rays were performed by Sakai and Ono,[83] who used 122-keV gamma rays from a radioactive Co^{57} source. This showed that magnetic Compton scattering could be observed and used to investigate the momentum distribution of polarized electrons in a crystal (see also Refs. 84 and 85, in which circularly polarized synchrotron radiation was employed). A more detailed theory of magnetic Compton scattering by bound electrons is given in Refs. 86 and 87.

We now turn to a more detailed examination of coherent elastic scattering, in which the atomic system remains in its initial state after the scattering event.[24–27,33] Here, we can use the nonrelativistic Hamiltonian for the interaction between the electron and the electromagnetic field:

$$H_1 = \frac{e^2}{2mc^2}\mathbf{A}^2 - \frac{e}{mc}\mathbf{pA} - [\boldsymbol{\mu}\mathbf{H}] = \frac{e^2}{2mc^2}\mathbf{A}^2 - \frac{e}{mc}\mathbf{p}'\mathbf{A}, \quad (2.21)$$

where $\mathbf{p}' = \mathbf{p} + (mc/e)[\boldsymbol{\mu}\nabla]$, $\mathbf{p}$ and $\boldsymbol{\mu}$ are the momentum and magnetic moment operators of the electron, and $\mathbf{A}$ is the vector potential of the field. The term containing $\mathbf{A}^2$ is responsible for Thomson scattering in first-order perturbation theory and the term $p'\mathbf{A}$ gives the dispersion corrections to the scattering amplitude in the second approximation.

This automatically includes magnetic scattering:[33]

$$\Delta f = \left(\frac{e}{mc}\right)^2 \sum_{m,s}\left[\frac{\langle 0|\mathbf{p}^{s'}\mathbf{A}_1^*|m\rangle\langle m|\mathbf{p}^{s'}\mathbf{A}_0|0\rangle}{E_0 - E_m + \hbar\omega - (i\Gamma_m/2)} + \frac{\langle 0|\mathbf{p}^{s'}\mathbf{A}_0|m\rangle\langle m|\mathbf{p}^{s'}\mathbf{A}_1^*|0\rangle}{E_0 - E_m - \hbar\omega}\right] \quad (2.22)$$

[cf. (2.1)]. A detailed analysis of magnetic scattering based on both (2.21) and with allowance for higher order relativistic corrections is given in Refs. 26 and 27.

As an example, consider the case of high frequencies, for which $\hbar\omega \gg (E_m - E_0)$. Summation over intermediate states $|m\rangle$ can then be carried out in (2.22) in an elementary manner, and Δf contains two terms (spin and orbital) that depend on the vectors $\mathbf{S}$ and $\mathbf{P}$, respectively:

$$\Delta f = r_e\left(\frac{\mathbf{PC}}{mc} - i\frac{\hbar\omega}{mc^2}\mathbf{SB}\right), \quad (2.23)$$

where

$$\mathbf{P} = \left\langle 0\left|\sum_s e^{i\mathbf{kr}_s}\mathbf{p}^s\right|0\right\rangle, \quad \mathbf{S} = \left\langle 0\left|\sum_s e^{i\mathbf{kr}_s}s^s\right|0\right\rangle,$$

$$\mathbf{C} = \mathbf{e}_0(\hat{\mathbf{k}}_0\mathbf{e}_1^*) + \mathbf{e}_1^*(\hat{\mathbf{k}}_1\mathbf{e}_0), \quad \mathbf{B} = [\mathbf{e}_1^*\mathbf{e}_0] + [\hat{\mathbf{k}}_1\mathbf{e}_1^*](\hat{\mathbf{k}}_1\mathbf{e}_0) - [\hat{\mathbf{k}}_0\mathbf{e}_0](\hat{\mathbf{k}}_0\mathbf{e}_1^*) - [[\hat{\mathbf{k}}_1\mathbf{e}_1^*][\hat{\mathbf{k}}_0\mathbf{e}_0]], \quad \mathbf{k} = \mathbf{k}_1 - \mathbf{k}_0.$$

The significant point here is that the spin and orbital terms have different dependence on both the polarizations $\mathbf{e}_0$ and $\mathbf{e}_1$ and the directions $\hat{\mathbf{k}}_0 = \mathbf{k}_0/|\mathbf{k}_0|$ and $\hat{k}_1 = \mathbf{k}_1/|\mathbf{k}_1|$ of the incident and scattered beams, so that we can separate out the contribution due to these terms and extract magnetic scattering against the background of Rayleigh scattering. For example, in general, magnetic scattering is different for right- and left-polarized beams, so that, when this is taken into account, the σ and π polarizations are no longer the eigenpolarizations, and so on. A more detailed analysis of the polarization properties of magnetic scattering can be performed in precisely the same way as in Sec. 2.3 (see also Ref. 88). We note that, from the practical point of view, the kinematic theory almost always suffices for the description of magnetic diffraction (because of the presence of absorption) although the dynamic analysis has also been carried out.[89,90]

Magnetic scattering of x-rays will undoubtedly become, in the immediate future, the working method for the investigation of the magnetic properties of solids. Despite the fact that the cross section for magnetic scattering of x-rays is lower by 4–5 orders of magnitude than the cross section for magnetic scattering of neutrons, this difficulty can be overcome by the high intensity of radiation delivered by synchrotron sources.[91] Thus, while the pioneering work[25,92] on the observation of magnetic reflections in NiO and Fe_2O_3, using ordinary x-ray tubes, required enormous effort (Ref. 93), the use of synchrotron sources has resulted in the investigation of even the details of magnetic structure. As an example, we may cite the investigation of the helical magnetic structure of holmium.[28,94–96] Additional reflections (satellites) appear near the crystal reflections in this case because the pitch of the helix is much greater than the lattice constant. These satellites were investigated in Refs. 28 and 90 and were found to be both magnetic scattering and magnetoelastic effects. The two can be separated on the basis of polarization properties.[28,88] The detailed investigation of positions, widths, and polarizations of these satellites, performed in Refs. 28 and 94–96, has revealed a number of nontrivial properties of magnetic ordering in holmium.

Apart from magnetic scattering, the x-ray region reveals the presence of magnetic dichroism and birefringence and, in particular, magnetic rotation of the plane of polarization (Faraday effect). These phenomena are described by

magnetic corrections to x-ray susceptibility that are proportional to the magnetic corrections to the forward-scattering amplitude of magnetic atoms. It is readily verified that the approximation used to derive (2.23) is then insufficient because the amplitude (2.23) vanishes for forward scattering.[82,97] Nonzero effects are obtained either in the case of higher-order corrections (of the order of $\alpha^2 = (e^2/\hbar c)^2$) or in the resonance case (near the absorption edge) when the dispersion correction becomes significant. The former case has been examined theoretically by Baryshevskiĭ *et al.*[98] (see also Ref. 82) and the results provide a quantitative description of the Faraday rotation of gamma rays with energies of about 200 keV (Ref. 99). For the x-ray range, (CuKα), theory predicts a rotation of the plane of polarization in iron by approximately 0.008 deg/cm, whereas the most recent experiments indicate an upper limit in iron of less than 50 deg/cm (Ref. 38). The observed rotation in nickel is of the order of 2–5 deg/cm (Ref. 4). The dispersion corrections[100–104] may be more significant in the x-ray range. Partially circularly polarized synchrotron radiation has been used[103] to show that circular dichroism in iron undergoes a considerable change (including a change of sign) near the absorption edge, and may reach 5×10^{-4} in the immediate neighborhood of the edge (≈ 10 eV) for a thickness of 2 mg/cm^2, i.e., 12.5 μm. A dichroism of the order of 10^{-4} has been seen in the EXAFS region (≈ 100 eV). Since dichroism is observed in the form of individual bands, it follows from the dispersion relations that the rotation of the plane of polarization in these bands should be of the same order as dichroism, i.e., cm^{-1} deg/cm.

Magnetic scattering of x-rays has a number of advantages in the study of magnetic properties as compared with neutron scattering (the latter is discussed in Ref. 105). For example, synchrotron sources can be used to achieve better resolution in k space (10^{-4} Å^{-1} is in prospect), which is particularly important in the study of long-period structures.[27,28,94–96] Resonance effects have particular advantages, e.g., in the selective investigation of the magnetic properties of atoms of a particular species, including the magnetic properties of unfilled states. Polarization measurements can be used to separate spin from orbital contributions to magnetization distributions and, in the case of resonance effects, to examine the structure of atomic and crystal states.[26,88,106–108] In the EXAFS region, magnetic scattering and dichroism are a source of information about the magnetic structure of the nearest-neighbor environment of an atom (the atom itself may, in fact, be nonmagnetic). We recall that oscillations in EXAFS arise because of the back scattering of photoelectrons, which depends on the spin of the photoelectron and on the magnetic moment of the scattering atom. Additional information can be obtained from the interference of magnetic scattering with Rayleigh scattering and the above scattering by the anisotropic part of the x-ray susceptibility. Particularly promising is the use of x-rays for the investigation of the magnetic structure of thin films, surfaces, and separation boundaries in solids.[27,109,110]

To conclude this Section, we note that successful investigations of the anisotropy of x-ray susceptibility and magnetic scattering will depend on advanced polarization measurement techniques, especially circular polarization measurements.

3. Polarization effects in x-ray-optical components. In this Section, we examine methods of producing and transforming the polarization of x-rays. Since polarization transforming devices are based on diffraction effects, our entire presentation will rest on the theory given in Section 1.

3.1. Polarization of radiation produced by x-ray sources. Traditional x-ray sources, i.e., x-ray tubes, produce either bremsstrahlung or characteristic radiation. It is well known that the former is polarized,[18,33] but its degree of polarization is relatively low because the direction of motion of electrons emitted by the cathode rapidly becomes isotropic as the electrons enter the solid target. The radiation is partially polarized along the electron beam. The degree of polarization amounts to only a few percent and increases toward shorter wavelengths.[111] The characteristic emission of polycrystalline targets is unpolarized. Single crystal produce partially polarized characteristic x-rays (especially in the L and M series), and this serves as a source of information about the anisotropy of the environment of atoms, their chemical bonds, and so on (see, for example, Ref. 112), but these effects are not used to produce polarized radiation. All this means that x-rays from conventional x-ray tubes are usually polarized by diffraction-based devices capable of producing only linear polarization (see below).

The godsend for x-ray optics has been the advent of synchrotron sources in which the radiation is emitted by electrons traveling with ultrarelativistic velocities in a magnetic field.[113–116] Synchrotron radiation from storage rings and wigglers has enormous intensity and a continuous spectrum. It is confined mostly to the orbital plane of the electrons (the divergence in the direction perpendicular to the oribtal plane is of the order of $mc^2/E \sim 10^{-4}$ at energies of approximately 5 GeV) and has unique polarization properties. In particular, the synchrotron radiation emitted by an electron traveling on a circular trajectory is 100% linearly polarized in the plane of the orbit, and its electric vector lies in this plane. Below and above the plane of the orbit (within the divergence angle $\Delta\psi$ at right-angles to the plane of the orbit), the radiation is right or left elliptically polarized depending on the sign of the projection of the direction of emission onto the angular velocity of the electron. The intensity distribution is shown in Fig. 13 for the linear and circular components of synchrotron radiation. Radiation with a high degree of circular polarization can be produced in specially designed wigglers.[117]

Exceptional possibilities for the production of polarized radiation with predetermined type and degree of polarization are provided by special device for generating synchrotron radiation, namely, undulators[116,118–119] (although we note that it is technically difficult to produce sufficiently hard x-ray radiation in these devices[120]). In planar undulators, mounted in the straight gaps of electron storage rings, the radiation is always linearly polarized. In helical undulators, the electrons move on helices and the radiation is circularly polarized. It has been suggested [121–123] that two planar undulators, rotated and shifted relative to one another, could be used. The coherent combination of two phase-shifted linearly polarized waves in this system of undulators can produce practically any polarization that can be varied in the course of an experiment. We also note that the radiation emitted by particles channelled in crystals is essentially similar to undulator radiation (Refs. 124–126).

The synchrotron radiation emitted by existing accelera-

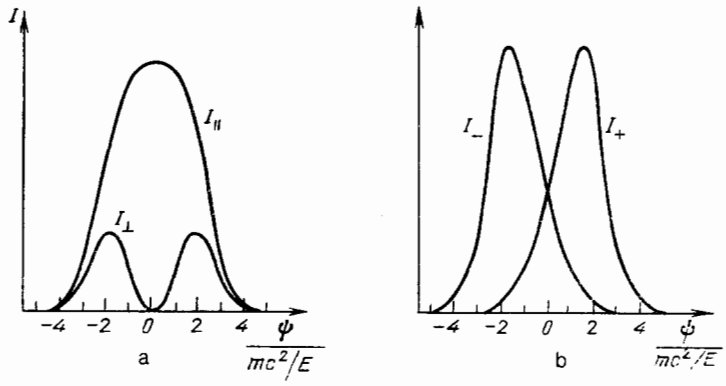

FIG. 13. Intensity of linear (a) and circular (b) polarization components of synchrotron radiation as functions of angle.

tors is partially depolarized because of the finite size of the beam and the spread in the direction of motion of electrons.[127–129] Crystal monochromators are another sourse of repolarization.[130] We note that, because of the difference between the reflection of σ- and π-polarized x-rays, crystal monochromators can be used to alter the polarization of synchrotron radiation, for example, elliptic polarization can be trimmed down to circular polarization. However, as discussed in detail in Sec. 1, it must be remembered that diffraction produces an additional phase differences between the σ and π components, and partial repolarization may take place (kinematic diffraction is an exception). These effects can be estimated and quantitatively taken into account by using the formulas given in Sec. 1, but, in the case of imperfect crystal monochromators, these estimates are not very reliable because, as a rule, the quantitative parameters describing the imperfections of crystal monochromators are not accurately known.

3.2. Production and analysis of linear polarization. Since most x-ray sources do not produce completely polarized radiation, diffraction-based polarization phenomena are widely used to produce, analyze, and transform polarized beams. Diffraction polarizers (and the corresponding analyzers) with $2\Theta_B = 90°$ are the most widely used (Refs. 2–5, 10–14, and 131–133) although the most promising polarizers are probably those based on dynamic diffraction effects, such as the Borrmann effect,[129,134,135] and the different widths of the Bragg reflection regions for π and σ polarizations[136–138] (another possibility is based on the spatial separation of σ- and π-polarized reflected beams[139]). The advantage of the 90° polarizer is its simplicity and the fact that the ability to scatter at 90° exclusively σ-polarized radiation does not depend on the degree of perfection or the thickness of the crystal. The disadvantage of these polarizers is that a crystal and a reflection with $2\Theta_B = 90°$ must be chosen for each wavelength. Moreover, for $\lambda \approx 1$ Å, the reflections are found to be of relatively higher order (for example, 333 in Ge in the case of CuKα radiation), so that their intensity is relatively low, which reduces the luminosity of the polarizer.

Polarizers based on the Borrmann effect (anomalous transmission effect) exploit the fact that the absorption of Bloch waves in the diffraction region is very different from the absorption of a plane wave. The difference is due to the fact that Bloch waves, which are superpositions of two or more plane waves, form a standing wave in the crystal. The absorption of this type of standing wave depends on whether its nodes occur at atoms or between them (in the former case, the absorption is greater and, in the second, significantly lower). The important point for us is that, for σ polarization, we can select conditions under which the Bloch wave field can be made to vanish at points occupied by the atoms, whereas this cannot be done for the π polarization because the π-polarization vectors have different directions for the direct and diffracted waves, and complete cancellation cannot be achieved. This means that the π-polarized component is absorbed to a greater extent even under the conditions of anomalous transmission, so that, by selecting a thick enough crystal, we can achieve complete σ polarization of both the transmitted and diffracted beams (in the Laue case). The main advantage of this method is that the Borrmann effect is observed for all Θ_B and can readily be wavelength tuned. Moreover, the effect is particularly well defined for strong reflections. The disadvantages are as follows: (a) high-quality crystals have to be employed; (b) for small Θ_B, the anomalous absorption coefficients for σ and π polarizations are not very different and one has to use thick crystals, which leads to absorption also of the "useful" σ-polarization, and (c) the Borrmann effect appears in a small reflection region with angular dimensions $\lesssim 1''$. All this restricts the range of application of polarizers based on the Borrmann effect.

The Hart-Rodrigues polarizers[136,137] are probably the most promising. They are based on the difference between the Bragg reflection widths for σ- and π-polarized beams (see Fig. 1a). These polarizing monochromators consist of two almost parallel crystals offset by an angle $\Delta\Theta$, greater than the Bragg reflection range for the π-polarized beam, but less than that for the σ-polarized beam. The π-polarization is significantly reduced (Fig. 14) after two successive reflections from the crystals. Any desired suppression of π-polarization can be achieved in principle by multiple reflection.[136] In practice, the Hart-Rodrigues polarizers are cut from one single crystal and the offset angle $\Delta\Theta$ is conveniently produced by controlled elastic deformation (Fig. 15). The polarizers are readily wavelength-tunable, and only a few Bragg reflections are sufficient to cover the entire x-ray range usually employed. The advantage of multiple reflections results from a number of causes including (a) the suppression of the "tails" of reflection curves, (b) higher harmonics ($\lambda/2$, $\lambda/3$,...) are found to appear and have a narrower Bragg reflection range, (c) when the number of reflections is even, there is no change in the direction of propagation of the beam, which is frequently convenient in x-ray optical measurements, and (d) the π-polarization is suppressed even in the absence of the crystal offset.

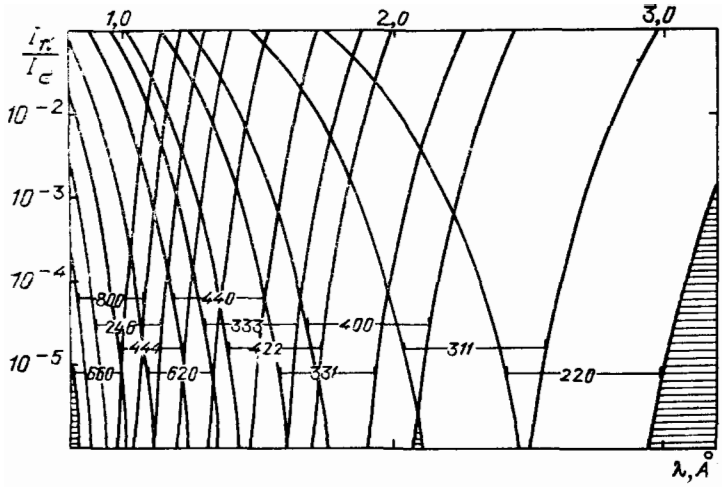

FIG. 14. Polarization ratio $|R_{\pi\pi}|^2/|R_{\sigma\sigma}|^2$ achieved with the Hart-Rodrigues polarizer after four reflections in Si (different reflections with the indices as shown are conveniently used in different wavelength ranges).[136]

We note that all the diffraction-based polarizers have the common and significant disadvantage that the angular divergence of the polarized beam is small in the direction perpendicular to the direction of polarization (it is of the order of the angular width of the Bragg reflection region), whereas the divergence in the direction of polarization is usually greater and is determined by the divergence of the incident beam. This difference must be taken into account in diffraction experiments with polarized beams, in which it can be a source of systematic uncertainty (a detailed analysis of three-crystal diffraction systems is given in Ref. 140). The system with crossed polarizer and analyzer, examined in detail by Hart,[3] is free from many of the systematic uncertainties and is capable of increasing the precision of polarization measurements.

3.3. The x-ray quarter-wave plate. Despite the fact that practically any polarization can be produced by using synchrotron or undulator radiation, there is a problem of producing and, especially, analyzing arbitrary polarized x-ray beams, including the transformation of linear into circular polarization and vice versa, i.e., there is the problem of producing a quarter-wave plate. As already noted, ordinary birefringence is very small in the x-ray region and great hopes are invested in the use of birefringence in the Bragg diffraction region (Sec. 1). These hopes have been realized experimentally.[3,85,103,141,142] We note, however, that the implementation of this idea directly in the strong diffraction scattering region encounters a number of practical difficulties. The main difficulty is that, because of the strong change in phases and intensities in the diffraction region (Figs. 1 and 2), beams with a very small $\lesssim 1''$ angular divergence have to be employed if a high degree of polarization is to be produced. In Sec. 1, we have already drawn attention to the fact that diffractive birefringence decreases relatively slowly as the direction of propagation of the beam deviates from the Bragg angle. We shall show that the use of this birefringence outside the region of strong diffractive reflection offers us a real possibility of transforming the polarization of a beam transmitted by a crystal and, in particular, of producing a quarter-wave plate.[7-9]

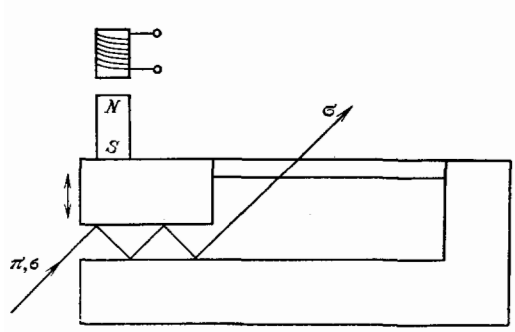

FIG. 15. The Hart-Rodrigues polarizer.[136]

The magnitude of birefringence, δn, in this angular range is given by (1.17) in both Laue and Bragg cases, and the intensity of the diffracted wave is very low (of the order of $|\chi_{\mathbf{H}}/\Delta\Theta|^2$). It follows that, in this case, the situation is, in many ways, analogous to the ordinary optics of anisotropic media, except that the magnitude of birefringence is very dependent on the direction of wave propagation.

The birefringence (1.17) ensures that the phase difference $\Delta\varphi = 2\pi \mathrm{Re}(\delta n)L/\lambda$ is established between the σ- and π-polarized components as the primary wave propagates through the medium (L is the path length in the crystal). A wave with linear polarization at 45° to the σ and π vectors is transformed into a circularly polarized wave for $\Delta\varphi = \pm\pi/2$, i.e., for $L_c = \lambda/|4\mathrm{Re}(\delta n)|$.

In order that this birefringence can actually be used to transform polarization, we must ensure that absorption should not be too large within the path length L_c, i.e.,

$$\mu L_c \equiv \frac{\mu\lambda\Delta\Theta_c}{\sin 2\Theta_B \,\mathrm{Re}\,(\chi_{\mathbf{H}}\chi_{\bar{\mathbf{H}}})} \lesssim 1 \qquad (3.1)$$

where μ is the absorption coefficient. Since χ_H is a function of Θ_B (via the atomic factor), there must be an optimum angle for (3.1) to be satisfied, and this can be found from the condition for $\mathrm{Re}(\chi_{\mathbf{H}}\chi_{\bar{\mathbf{H}}})\sin 2\Theta_B$ to be a maximum. Next, since $\mu \sim Z^4$ and $\chi_{\mathbf{H}} \sim Z$ (Z is the atomic number), it is convenient to use crystals with low Z atoms to satisfy (3.1).

As an example, consider the propagation of CuKα radiation ($\lambda = 1.54$ Å) in diamond near the 111 reflection. Using (1.17), we find that $L_c = 2.6\cdot 10^2\,\Delta\Theta_c$, where L_c is in centimeters and $\Delta\Theta_c$ in radians. When $\Delta\Theta_c = 0.5' = 1.45\cdot 10^{-4}$, we have $L_c = 0.038$ cm and $\exp(-\mu L_c) = 0.5$. In the wavelength range between about 3 Å and 0.5 Å, the difference $\Delta\Theta_c$ for which $\mu L_c = 1$ is found to change from $\Delta\Theta_c \approx 1'$ to $\Delta\Theta_c \approx 0.13'$, respectively,

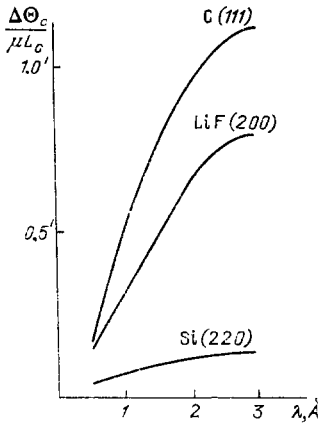

FIG. 16. The difference $\Delta\Theta_c$ as a function of wavelength, calculated for the quarter-wave plate for different reflections (the angular difference $\Delta\Theta_c$ can be increased by increasing the plate thickness L_c).

and the conditions for the validity of this approximation are well satisfied (the intensity of the diffracted wave is less than 1% of the incident intensity). Similar results are obtained for the 220 and 200 reflections in LiF (Fig. 16); in silicon, $\Delta\Theta_c \sim 1'$ for $\mu L_c \sim 5$–10.

We must now consider the effect of a significant angular divergence of the beam (the fact that the beam is not monochromatic can be taken into account similarly). Because of this divergence, the Bragg reflection range $\Delta\Theta$ is not strictly fixed so that the wave transmitted by the crystal is a superposition of waves with different polarizations, i.e., it is partially polarized. Suppose that the wave incident on the crystal has a linear polarization at 45° to the σ and π vectors, the deviation from the Bragg angle ranges from $\Delta\Theta_c - (\Delta\Theta'/2)$ to $\Delta\Theta_c + (\Delta\Theta'/2)$, and all the angles on this interval have equal probability. The mean deviation $\Delta\Theta_c$ is chosen so that the transformation of linear polarization into circular polarization occurs within this difference. It can then be shown that the degree of polarization in this case is given by

$$P = \left| \int_{-1/2}^{1/2} \exp\left(i \frac{\pi}{2} \frac{\Delta\Theta_c}{\Delta\Theta_c + x\Delta\Theta'} \right) dx \right|. \qquad (3.2)$$

When $\Delta\Theta' \ll |\Delta\Theta_c|$, we can readily show from this that, very approximately,

$$P = 1 - \frac{\pi^2}{96}\left(\frac{\Delta\Theta'}{\Delta\Theta_c}\right)^2. \qquad (3.3)$$

It follows from this expression that $\Delta\Theta'$ need not be too small in comparison with $|\Delta\Theta_c|$. Even for $\Delta\Theta' \approx 0.5|\Delta\Theta_c|$, the polarization calculated from (3.2) is found to be quite high: $P \approx 0.97$.

We may therefore conclude that the transformation of x-ray polarization (including linear into circular polarization and vice versa) can be carried out with a small loss of intensity. It is important to note that the case we have considered has a number of advantages from the practical point of view, and these are not available when birefringence is used directly in the strong diffraction region. Actually, the diffraction correction to the refractive index varies rapidly within the Bragg reflection range (Figs. 1 and 2) and the necessary condition for producing a given polarization is that the divergence $\Delta\Theta'$ of the incident beam must be much less than the angular width of the Bragg reflection range, i.e., it must be of the order of a fraction of a second of arc. On the other hand, in the case we are considering, we have to satisfy the less stringent inequality $\Delta\Theta' \ll |\Delta\Theta_c|$, which is in fact more readily satisfied because $|\Delta\Theta_c|$ can be of the order of a few minutes of arc. Moreover, there are several complicating factors in the diffraction region (Sec. 1), including the presence of several waves, the Borrmann effect, and so on, whereas, in our case, the situation is similar to that in ordinary optics.

A further advantage of this approach is that, outside the Bragg reflection region, birefringence is not very dependent on the degree of perfection of the crystal (Sec. 1). The above expressions can therefore be used even for relatively imperfect crystals, provided the deviation from the Bragg angle is much greater than the width of the reflection curve.

To conclude this section, we note that elliptic polarization can be obtained from linear polarization by diffraction in the Bragg geometry if we use the phase difference between diffracted waves with σ and π polarizations (Fig. 1a).[143,144] However, the practical implementation of this idea encounters a number of difficulties. For example, several successive reflections are necessary to produce circular polarization in this geometry.[143]

3.4. Pendellösung. This is one of the well-defined dynamic effects arising as a result of interference between Bloch waves. We recall (Sec. 1) that, for each polarization (σ and π), there are two Bloch eigenwaves with different wave vectors. This difference gives rise to intensity beats (Pendellösung) in both the waves transmitted by the crystal and in the diffracted waves [(1.7) and (1.8)]. These beats can be observed, depending on the angle of deviation from the Bragg conditions and the path traversed in the crystal. The beats in the dependence on the crystal thickness occur even in the integrated parameters (Figs. 2 and 3). The significant point is that, because of the difference between the scattering amplitudes for σ- and π-polarized waves, the oscillation periods for these two polarizations are different, and this can give rise to the mutual extinguishing of the oscillations[34,145,146] if the incident radiation is unpolarized or circularly polarized or polarized at an angle of 45° to the σ and π polarizations. It is well known that the above beats can be used in the precise measurement of structure amplitudes. It is therefore desirable to use σ- or π-polarized radiation to increase the contrast of the interference pattern (and the precision with which the structure amplitudes can be measured).[147]

Pendellösung is also observed in the polarization characteristics of beams,[2] such as the angle of rotation and the ratio of the axes of the polarization ellipse (if the polarization of the incident beam is different from σ or π), but the beats are less well defined in the degree of polarization.

To conclude this Section, let us briefly enumerate applications of polarized x-rays that were not mentioned above. First, there is the topography of almost perfect crystals. In this case, small distortions of the lattice can be observed if the width of the reflection curve is as small as can be achieved by using π-polarized radiation (it is shown in Ref. 148 that a relative distortion of the lattice of the order of 10^{-8} can be observed). The diffraction of π-polarized radiation for angles $2\Theta_B$ approaching 90° can be used to elimi-

nate extinction in the case of precise measurements of structure amplitudes.[149,150] The absence of scattered π-polarized radiation at 90° is also used to improve the signal-to-noise ratio in x-ray fluorescence analysis[151,152] and in Mössbauer filtration of synchrotron radiation.[153] There is no doubt that x-ray polarization phenomena will find new applications and will be extended still further.

Conclusion. X-ray polarization phenomena and their applications (both possible and already implemented) that we have discussed show that this method of investigating the properties of solids is informative and promising. Although the practical implementation of the method involves increasingly complicated equipment (including synchrotron sources), all this is justified by the unique character of the data obtained in this way. A clearer picture of possible future developments in this area can be obtained by enumerating some of the unsolved problems. They include, above all, the complete polarization measurement on x-ray beams, i.e., the determination of all three polarization parameters, namely, the degree of polarization, orientation, and ratio of the axes of the polarization ellipse. At present, the main difficulty is to produce and, especially, analyze circular polarization. This difficulty will be overcome once the quarter-wave plate, which is convenient to use in practice, has become available. "Forbidden" reflections, e.g., magnetic reflections and those connected with the anisotropy of susceptibility (Sections 2.3 and 2.4) can also be used to analyze circular polarizations. We note that the problem of complete polarizations measurement can be solved in the case of Mössbauer radiation, which also lies in the x-ray region. Polarizers and analyzers of arbitrary polarization have been developed for Mössbauer radiation.[154–158] X-ray polarization phenomena can also be investigated in ordinary (non-Mössbauer) crystals by using the Mössbauer detection technique in which the source of radiation is a Mössbauer source instead of the x-ray tube (the range of validity of this method is limited by the discrete character of the wavelength employed[159] and, mostly, by the low intensity of Mössbauer sources).

Polarization phenomena under the conditions of multiwave diffraction[160–165] have not been adequately investigated. When noncoplanar multiwave geometry is employed, the eigenpolarizations are almost always different from σ and π and, moreover, do not remain constant in the diffraction region. It may be expected, for example, that a particular circular polarization will be preferentially reflected, and there may be some other unusual effects. We also note that, in the case of noncoplanar multiwave diffraction by imperfect crystals, the equations for the polarization tensors have to be employed even when the intensities of diffracted waves are calculated. Studies of the polarization of x-ray beams in resonators[166–168] and in diffraction focusing[169–170] have only just begun. The polarization of x-rays that have undergone inelastic scattering or scattering by defects has not been adequately investigated. The polarization of Compton-scattered photons carries information on the momentum distribution of polarized electrons, whereas the polarization of diffusely scattered x-rays can be used to determine the presence of dynamic effects.[171] Relatively little attention has been devoted to polarization effects accompanying diffraction under the conditions of total external reflection.[172–175] Studies of the rotation of the plane of polarization of x-rays in optically active media have only just begun.[3,5,38,176] Certain technical problems remain unresolved, for example, there is no metrologic basis for polarization measurements in the x-ray range.[177,178] In view of the increasing number of available synchrotron sources, and advances in the techniques of traditional x-ray measurements, it is expected that there will be a rapid expansion in the study and application of polarization effects in x-ray optics, and rapid progress in the areas enumerated above.

The authors are indebted to M. A. Andreeva, V. A. Bushuev, V. M. Kaganer, A. V. Kolpakov, V. G. Labushkin, M. M. Nikitin, E. N. Ovchinnikova, and E. V. Smirnov for useful discussions.

[1)]Similar reflections are also possible in quasicrystals.

[2)]We note that as $\Delta\Theta$ tends to $\pm\infty$ in the Laue case, both the phase difference and the phase of wave transmitted by the crystal can have different limits $\varphi + \infty$ and $\varphi \to \infty$ that differ by $360°.N$, where N is an integer (see Fig. 2b). The number N is a topological invariant; it depends on the crystal thickness and changes by unity for thicknesses for which either $T_{\sigma\sigma}$ or $T_{\pi\pi}$ vanishes at some point in the interior of the diffraction region; if the crystal thickness is much less than the primary extinction length, then $N = 0$.

[3)]The translator is greatly indebted to Professor Michael Hart FRS for his expert advice.

[1]C. G. Barkla, Proc. R. Soc. London **77**, 247 (1906).
[2]I. P. Mikhaĭlyuk, S. A. Kshevetskiĭ, M. V. Ostapovich, and V. P. Shafranyuk, Ukr. Fiz. Zh. **22**, 61 (1977).
[3]M. Hart, Philos. Mag. Ser. B **38**, 41 (1978).
[4]J. Hrdý, E. Krouský, and O. Renner, Phys. Status Solidi A **53**, 143 (1979).
[5]Yu. V. Ponomarev and Yu. A. Turutin, Zh. Tekh. Fiz. **52**, 185 (1982) [Sov. Phys. Tech. Phys. **27**, 129 (1982)].
[6]L. V. Azaroff and D. M. Pease, *X-Ray Spectroscopy*, ed. by L. V. Azaroff, McGraw-Hill, N.Y., 1974, p. 284.
[7]N. B. Baranova and B. Ya. Zel'dovich, Zh. Eksp. Teor. Fiz. **79**, 1779 (1980) [Sov. Phys. JETP **52**, 900 (1980)].
[8]V. E. Dmitrienko and V. A. Belyakov, Pis'ma Zh. Tekh. Fiz. **6**, 1440 (1980) [Sov. Tech. Phys. Lett. **6**, 616 (1980)].
[9]V. A. Belyakov and V. E. Dmitrienko, Kristallografiya **27**, 14 (1982) [Sov. Phys. Crystallogr. **27**, 6 (1982)].
[10]S. Chandrasekhar, Adv. Phys. **9**, 363 (1960).
[11]N. M. Olekhnovich and V. L. Markovich, Kristallografiya **23**, 658 (1978) [Sov. Phys. Crystallogr. **23**, 369 (1978)].
[12]L. D. Jennings, Acta Crystallogr. A **24**, 584 (1968).
[13]N. M. Olekhnovich, Izv. Akad. Nauk BSSR Ser. Fiz.-Mat. Nauk. No. 4, 57 (1980).
[14]N. M. Olekhnovich, Polarization of Diffraction and the Dynamic Scattering of X-Rays in Real Crystals, Thesis for the Degree of Doctor of Phys. Math. Sciences [in Russian], Kiev, 1987.
[15]V. E. Dmitrienko and V. A. Belyakov, Acta Crystallogr. A **36**, 1044 (1989).
[16]S. Chandrasekhar, *Radiative Transfer*, Clarendon Press, Oxford, 1950 [Russ. Transl., IL, M., 1953].
[17]G. V. Rozenberg, Usp. Fiz. Nauk. **56**, 77 (1955); **121**, 97 (1977) [Sov. Phys. Usp. **20**, 55 (1977)].
[18]V. L. Ginzburg, *Theoretical Physics and Astrophysics*, Pergamon Press, Oxford, 1979 [Russ. original Nauka, M., 1975 latered., 1981].
[19]Yu. N. Barabanenkov, Usp. Fiz. Nauk. **117**, 49 (1975) [Sov. Phys. Usp. **18**, 673 (1975)].
[20]D. H. Templeton and L. K. Templeton, Acta Crystallogr. A **36**, 237 (1980); **41**, 133 (1985).
[21]D. H. Templeton and L. K. Templeton, *ibid.* **42**, 478 (1986).
[22]V. E. Dmitrienko, *ibid.* **39**, 29 (1983).
[23]V. E. Dmitrienko, *ibid.* **40**, 89 (1984).
[24]P. M. Platzman and N. Tzoar, Phys. Rev. B **2**, 3556 (1970).
[25]F. DeBergevin and M. Brunel, Acta Crystallogr. A **37**, 314 (1981); M. Brunel and F. DeBergevin, *ibid.* 324.
[26]O. L. Zhizhimov and I. B. Khriplovich, Zh. Eksp. Teor. Fiz. **87**, 547 (1984) [Sov. Phys. JETP **60**, 313 (1984)].
[27]M. Blume, J. Appl. Phys. **57**, 3615 (1985).
[28]D. Gibbs, D. E. Moncton, K. L. D'Amico, J. Bohr, and B. H. Grier, Phys. Rev. Lett. **55**, 234 (1985).
[29]V. I. Iveronova and G. P. Revkevich, *Theory of X-Ray Scattering* [in Russian], Moscow University, 1978.
[30]J. M. Cowles, *Diffraction Physics*, North-Holland, Amsterdam [Russ. Transl., Mir, M., 1979].

[31]Z. G. Pinsker, *X-Ray Crystal Optics* [in Russian], Nauka, Moscow, 1982.
[32]B. K. Vaĭnshteĭn, Modern Crystallography, Springer-Verlag, Berlin, 1981 [Russ. original Nauka, M., 1979, Vol. 1].
[33]A. I. Akhiezer and V. B. Berestetskiĭ, *Quantum Electrodynamics*, Interscience, N.Y., 1965. [Russ. original, Nauka, M., 1964 and 1969].
[34]P. Scalicky and C. Malgrange, Acta Crystallogr. A **28**, 501 (1972).
[35]S. Annaka, J. Phys. Soc. Jpn. **51**, 1927 (1982).
[36]S. Annaka, T. Suzuki, and K. Onoue, Acta Crystallogr. A **36**, 151 (1980).
[37]G. G. Cohen and M. Kuriyama, Phys. Rev. Lett. **40**, 957 (1978).
[38]M. Hart and A. R. D. Rodrigues, Philos. Mag. Ser. B **43**, 321 (1981).
[39]C. G. Darwin, Philos. Mag. **43**, 800 (1922).
[40]W. H. Zachariasen, Acta Crystallogr. **23**, 558 (1987).
[41]P. Becker, *ibid.* Sec. A **33**, 243 (1977).
[42]V. E. Dmitrienko, Kristallografiya **27**, 213 (1982) [Sov. Phys. Crystallogr. **27**, 131 (1982)].
[43]V. E. Dmitrienko and V. A. Belyakov, Zh. Eksp. Teor. Fiz. **73**, 681 (1977) [Sov. Phys. JETP **46**, 356 (1977)].
[44]S. Ramasechan and G. N. Ramachandran, Acta Crystallogr. **6**, 364 (1953).
[45]S. Chandrasekhar, *ibid.* **9**, 954 (1956).
[46]K. S. Chandrasekharan, *ibid.* **12**, 916 (1959).
[47]N. M. Olekhnovich, Kristallografiya **14**, 840 (1969) [Sov. Phys. Crystallogr. **14**, 724 (1970)]; **18**, 1240 (1973); Dokl. Akad. Nauk. SSSR **213**, 560 (1973) [Sov. Phys. Dokl. **18**, 728 (1973)]; Dokl. Akad. Nauk SSSR **18**, 696 (1974).
[48]N. M. Olekhnovich and M. P. Shmidt, Izv. Akad. Nauk SSSR Ser. Fiz. Mat. Nauk. No. 4, 115 (1974); No. 4, 110 (1975); No. 1, 118 (1977).
[49]N. M. Olekhnovich, V. A. Rubtsov, and M. P. Shmidt, Kristallografiya **20**, 796 (1975) [Sov. Phys. Crystallogr. **20**, 488 (1975)].
[50]N. M. Olekhnovich, V. L. Markovich, and A. I. Olekhnovich, Acta Crystallogr. A **36**, 989 (1980).
[51]N. M. Olekhnovich, V. L. Markovich, and A. I. Olekhnovich, Kristallografiya **27**, 886 (1982) [Sov. Phys. Crystallogr. **27**, 533 (1982)]; N. M. Olekhnovich, A. L. Karpeĭ, and A. I. Olekhnovich, Izv. Akad. Nauk. BSSR Ser. Fiz.-Mat. Nauk. No. 5, 43 (1983).
[52]N. M. Olekhnovich and A. V. Pushkarev, Dokl. Adad. Nauk BSSR **29**, 38 (1985).
[53]N. M. Olekhnovich, A. L. Karpeĭ, and V. L. Markovich, Krist. Tech. **13**, 1463 (1978); N. M. Olekhnovich and A. V. Pushkarev, Izv. Akad. Nauk BSSR Ser. Fiz.-Mat. Nauk No. 6, 53 (1983).
[54]N. Kato, Acta Crystallogr. A **32**, 453, 458 (1976); **35**, 9 (1979); **36**, 171, 763, 770 (1980).
[55]S. P. Darbinyan, I. A. Vartan'yants, and F. N. Chukhovskiĭ, Fizika No. 8–9 67 (1987).
[56]V. A. Bushuev, Kristallografiya **34**, 279 (1989) [Sov. Phys. Crystallogr. **34**, 163 (1989)].
[57]L. D. Jennings, Acta Crystallogr. A **37**, 584 (1981); **40**, 12 (1984).
[58]Y. Le Page, E. J. Gabe, and L. D. Calvert, J. Appl. Crystallogr. **12**, 25 (1979); M. G. Vincent and H. D. Flack, *ibid.* **36**, 610, 614 (1980).
[59]A. McL. Mathieson, Acta Crystallogr. A **34**, 404 (1978); H. D. Flack and M. G. Vincent, *ibid.* 620; J. L. Lawrence, *ibid*, **38**, 859 (1982).
[60]A. V. Vinogradov and I. V. Kozhevnikov, Preprint FIAN SSSR No. 102 [in Russian], Moscow, 1987.
[61]A. V. Kolpakov, V. A. Bushuev, and R. N. Kuz'min, Usp. Fiz. Nauk **126**, 479 (1978) [Sov. Phys. Usp. **21**, 959 (1978)]; A. V. Kolpakov, E. N. Ovchinnikova, and R. N. Kuz'min, VINITI AN SSSR No. 155 [in Russian], Moscow, 1978.
[62]M. Born and E. Wolf, *Principles of Optics*, Pergamon Press, Oxford, 1975 [Russ. Transl. of an earlier edition, Nauka, M., 1970].
[63]L. D. Landau and E. M. Lifzhitz, *Electrodynamics of Continuous Media*, Pergamon Press, Oxford, 1984 [Russian original, Nauka, M., 1982].
[64]S. Ramaseshan and S. C. Abrahams (eds.), *Anomalous Scattering*, Munksgaard, Copenhagen, 1975.
[65]J. E. Hahn and K. O. Hodgson, *Inorganic Chemistry: Toward the 21st Century*, Washington, 1983, p. 431.
[66]D. H. Templeton and L. K. Templeton, Acta Crystallogr. A **41**, 365 (1985).
[67]G. A. Korn and T. M. Korn, *Mathematical Handbook for Scientists and Engineers*, McGraw-Hill, N.Y., 1961 [Russ. Transl. Nauka, M., 1978].
[68]A. V. Shubnikov and V. A. Koptsik, *Symmetry in Science and Art*, Plenum, N.Y., 1974 [Russ. original Nauka, M., 1972].
[69]V. A. Belyakov, Usp. Fiz. Nauk **115**, 553 (1975) [Sov. Phys. Usp. **8**, 267 (1975)].
[70]V. A. Belyakov, V. E. Dmitrienko, and V. P. Orlov, Usp. Fiz. Nauk **127**, 221 (1979) [Sov. Phys. Usp. **22**, 63 (1979)].
[71]*International Tables for X-ray Crystallography*, Kynoch Press, Birmingham, U.K., 1952.
[72]M. Renninger, Z. Phys. **106**, 141 (1937).
[73]B. Dawson, Proc. R. Soc. London **298**, 255, 264, 379 (1967).
[74]V. A. Belyakov, Fiz. Tverd. Tela (Leningrad) **13**, 3320 (1971) [Sov. Phys. Solid State **13**, 2789 (1972)].
[75]D. H. Templeton and L. K. Templeton, Acta Crystallogr. A **43**, 573 (1987).
[76]Yu. S. Terminasov and L. V. Tuzov, Usp. Fiz. Nauk **83**, 223 (1964) [Sov. Phys. Usp. 7, 434 (1964)].
[77]B. Post and J. Ladell, Acta Crystallogr. A **43**, 173 (1987).
[78]J. Z. Tischler, Q. Shen, and R. Colella, *ibid.* **41**, 451 (1985).
[79]E. K. Kov'ev and V. I. Simonov, Pis'ma Zh. Eksp. Teor. Fiz. **43**, 244 (1986) [JETP Lett. **43**, 312 (1986)].
[80]M. Gell-Mann and M. L. Goldberger, Phys. Rev. **96**, 1433 (1954).
[81]K. Namikawa, M. Ando, T. Nakajima, and H. Kawata, J. Phys. Soc. Jpn. **54**, 4099 (1985).
[82]F. E. Low, Phys. Rev. **96**, 1428 (1954).
[83]N. Sakai and K. Ono, Phys. Rev. Lett. **37**, 351 (1976).
[84]M. J. Cooper, D. Laundy, D. A. Cardwell, D. N. Timms, R. S. Holt, and G. Clark, Phys. Rev. B **34**, 5984 (1986).
[85]D. M. Mills, *ibid.* **36**, 6178 (1987).
[86]P. M. Platzman and N. Tzoar, J. Appl. Phys. **57**, 3623 (1985).
[87]H. Grotch, E. Kazer, G. Bhatt, and D. A. Owen, Phys. Rev. A **27**, 243 (1983).
[88]S. W. Lovesey, J. Phys. C **20**, 5625 (1987).
[89]F. A. Babushkin, *Dynamic Theory of Magnetic Scattering of X-Rays by Antiferromagnetic Materials* [in Russian], Leningrad University, 1979.
[90]S. M. Durbin, Phys. Rev. A **36**, 639 (1987).
[91]P. M. Brunel, G. Patrat, *et al.*, Acta Crystallogr. A **39**, 84 (1983).
[92]F. DeBergevin and M. Brunel, Phys. Lett. A **39**, 141 (1972).
[93]N. N. Faleyev, A. A. Lomov, and V. G. Labushkin, Acta Crystallogr. Sec. A **37**, C-374 (1981).
[94]D. Gibbs, D. E. Moncton, and K. L. D'Amico, J. Appl. Phys. **57**, 3619 (1985).
[95]D. E. Moncton, D. Gibbs, and J. Bohr, Nucl. Instrum. Methods A **246**, 839 (1986).
[96]J. Bohr, D. Gibbs, D. E. Moncton, and K. L. D'Amico, Physica (Utrecht) A **140**, 349 (1986).
[97]V. Kamersky and J. Kaczer, Acta Phys. Slov. **30**, 329 (1980),
[98]V. G. Baryshevskiĭ, O. V. Dumbrais, and V. L. Lyuboshits, Pis'ma Zh. Eksp. Teor. Fiz. **15**, 113 (1972) [JETP Lett. **15**, 78 (1972)].
[99]V. M. Lobashov, L. A. Popeko, L. M. Smotritskiĭ, A. P. Serebrov, and E. A. Kolomenskiĭ, Pis'ma Zh. Eksp. Teor. Fiz. **14**, 373 (1971) [JETP Lett. **14**, 251 (1971)].
[100]B. T. Those, G. van der Laan, and G. A. Sawatzky, Phys. Rev. Lett. **55**, 2086 (1985).
[101]V. G. Baryshevskiĭ and S. A. Maksimenko, Opt. Spektrosk. **61**, 970 (1986) [Opt. Spectrosc. (USSR) **61**, 606 (1986)].
[102]G. van der Laan, B. T. Thole, G. A. Sawatzky, J. B. Goedkoop, J. C. Fuggle, J. M. Esteva, R. Karnatak, J. P. Remeika, and N. A. Dabkowska, Phys. Rev. B **34**, 6529 (1986).
[103]G. Schütz, W. Wagner, W. Wilhelm, P. Kienle, R. Zeller, R. Frahm, and G. Materlik, Phys. Rev. Lett. **58**, 737 (1987).
[104]J. B. Goedkoop, B. T. Thole, G. van der Laan, G. A. Sawatzky, F. M. F. de Groot, and J. C. Fuggle, Phys. Rev. B **37**, 2086 (1988).
[105]Yu. A. Izyumov, V. E. Naĭsh, and R. P. Ozerov, *Neutron Diffraction by Magnetic Materials* [in Russian], Atomizdat, M., 1981.
[106]M. Blume and D. Gibbs, Phys. Rev. B **37**, 1779 (1988).
[107]D. Gibbs, D. R. Harshman, E. D.Isaacs, D. B. McWhan, D. Mills, and C. Vettier, Phys. Rev. Lett. **61**, 1241 (1988).
[108]J. P. Hannon, G. T. Trammel, M. Blume, and D. Gibbs, *ibid.* 1245.
[109]M. Weinert, A. J. Freeman, S. Ohnishi, and J. Davenport, J. Appl. Phys. **57**, 3641 (1985).
[110]C. Vettier, D. B. McWhan, E. M. Gyorgy, J. Kwo, B. M. Buntschuh, and B. W. Batterman, Phys. Rev. Lett. **56**, 757 (1986).
[111]M. A. Blokhin, *Physics of X-Rays* [in Russian], Gostekhizdat, M., 1957.
[112]A. Maĭzel, G. Leonkhardt, and R. Sargan, *X-Ray Spectra and Chemical Bonds* [in Russian], Naukova Dumka, Kiev, 1981.
[113]G. N. Kulipanov and A. N. Skripskiĭ, Usp. Fiz. Nauk **122**, 369 (1977) [Sov. Phys. Usp. **20**, 559 (1977)].
[114]I. M. Ternov, V. V. Mikhaĭlin, and V. R. Khalilov, *Synchrotron Radiation and Its Applications* [in Russian], Moscow University, 1980.
[115]C. Kunz, (ed.), *Synchrotron Radiation*, Springer-Verlag, Berlin, 1979 [Russ. Transl., Mir, M., 1981].
[116]M. M. Nikitin and V. Ya. Epp, *Undulator Radiation* [in Russian], Energoatomizdat, M., 1988.
[117]J. Goulon, P. E. Elleaume, and D. Raoux, Nucl. Instrum. Methods A **254**, 192 (1987).
[118]D. F. Alferov, Yu. A. Bashmakov, and E. G. Bessonov, Tr. Fiz. Inst. Akad. Nauk SSSR **80**, 100 (1975) [Proc. (Tr.) P. N. Lebedev Phys. Inst. Acad. Sci. USSR **80** (1975)].
[119]D. F. Alferov, Yu. A. Bashmakov, and P. A. Cherenkov, Usp. Fiz.

Nauk **157**, 389 (1989) [Sov. Phys. Usp. **32**, 200 (1989)].
[120]E. S. Gluskin, S. V. Gaponov, S. A. Gusev, P. Dhez, P. P. Ilyinsky, Yu. Ya. Platonov, N. N. Salashchenko, and Yu. M. Shatunov, Preprint INP 83-163, Novosibirsk, 1983.
[121]M. B. Moiseev, M. M. Nikitin, and N. I. Fedosov, Izv. Vyssh. Uchebn. Zaved. Fiz. No. 3, 76 (1978) [Sov. Phys. J. No. 3 (1978)].
[122]K. J. Kim, Nucl. Instrum. Methods A **219**, 425 (1984).
[123]H. Onuki, *ibid.* **246**, 94 (1986).
[124]V. G. Baryshevskiĭ, Channeling, *Radiation and Reactions in Crystals at High Energies* [in Russian], Belorussian University, Minsk, 1982.
[125]M. A. Kumakhov, *Radiation by Channelled Particles in Crystals* [in Russian], Energoatomizdat, M., 1986.
[126]V. A. Bazylev and N. K. Zhevago, *Radiation by Fast Particles in Matter and in External Fields* [in Russian], Nauka, M., 1987.
[127]G. Materlik and P. Suortti, J. Appl. Crystallogr. **17**, 7 (1984).
[128]H. Derenbach, R. Malutzki, and V. Schmidt, Nucl. Instrum. Methods A **208**, 845 (1983).
[129]D. H. Templeton and L. K. Templeton, J. Appl. Crystallogr. **21**, 151 (1988).
[130]R. Caciuffo, S. Melone, F. Rustichelli, and A. Boeuf, Phys. Rep. **152**, 1 (1987).
[131]F. Riehle, Nucl. Instrum. Methods A **246**, 385 (1986).
[132]E. S. Gluskin, S. V. Gaponov, P. Dhez, P. P. Ilyinsky, N. N. Salashchenko, Yu. M. Shatunov, and E. M. Trakhtenberg, *ibid.* 394.
[133]P. Dhez, *ibid.* **261**, 66 (1987).
[134]H. Cole, F. W. Chambers, and C. G. Wood, J. Appl. Phys. **32**, 1942 (1961).
[135]J. L. Staudenmann, L. D. Chapman, W. J. Murphy, R. D. Horning, and G. L. Liedel, *ibid.* **18**, 519 (1985); J. L. Staudenmann, L. D. Chapman, *et al.*, *ibid.* 724.
[136]M. Hart and A. R. D. Rodrigues, Philos. Mag. Ser. B **40**, 149 (1979).
[137]M. Hart, Lect. Not. Phys. **112**, 325 (1980).
[138]G. G. Avetisyan, Izv. Akad. Nauk Arm. SSR Tekh. Nauk **39**, 47 (1986).
[139]A. V. Andreev, V. E. Gorshkov, and Yu. A. Il'inskii, Zh. Tekh. Fiz. **57**, 511 (1987) [Sov. Phys. Tech. Phys. **32**, 308 (1987)].
[140]J. Hrdý and E. Krouský, Czech. J. Phys. B. **23**, 966 (1973).
[141]J. A. Golovchenko, B. M. Kincaid, R. A. Levesque, A. E. Meixner, and D. R. Kaplan, Phys. Rev. Lett. **57**, 202 (1986).
[142]O. Brümmer *et al*, Z. Naturforsch. **37a**, 524 (1982).
[143]A. G. Grigoryan, P. A. Bezirganyan, and S. A. Aladzhadzhyan, All-Union Conf. on Methods and Equipment for Research into the Coherent Interaction Between Radiation and Matter. Abstracts. [in Russian], Institute of Atomic Energy, M., 1980, p. 66.
[144]O. Brümmer, Ch. Eisenschmidt, and H. R. Höche, Acta Crystallogr. Sec. A **40**, 394 (1985).
[145]H. Hattori, H. Kuriyama, and N. Kato, J. Phys. Soc. Jpn. **20**, 1047 (1965).
[146]M. Hart and A. R. Lang, Acta Crystallogr. **19**, 73 (1965).
[147]K. Utemisov, S. Sh. Shil'shteĭn, and V. A. Somenkov, Kristallografiya, **26**, 182 (1981) [Sov. Phys. Crystallogr. **26**, 101 (1981)].
[148]U. Bonse *et al.*, Nucl. Instrum. Methods A **208**, 711 (1983).
[149]A. Mathieson, Acta Crystallogr. Sec. A **33**, 133 (1984).
[150]W. B. Yelon and B. van Laar, *ibid.* **40**, 261 (1984).
[151]T. G. Duzubeg, B. V. Jarrett, and J. M. Jaklevic, Nucl. Instrum. Methods **115**, 297 (1974).
[152]R. W. Ryon and J. D. Zahrt, Adv. X-Ray Anal. **22**, 453 (1979).
[153]V. A. Belyakov, Usp. Fiz. Nauk **151**, 699 (1987) [Sov. Phys. Usp. **30**, 331 (1987)].
[154]V. G. Labushkin, S. N. Ivanov, and G. V. Chechin, Pis'ma Zh. Eksp. Teor. Fiz. 349 (1974) [JETP Lett. **20**, 157 (1974)].
[155]U. Gonser and H. Fisher, in *Mössbauer Spectroscopy II: The Exotic Side of the Method*, ed. by U. Gonser, Springer-Verlag, Berlin, 1981. [Russ. Transl., Mir, M., 1984, p. 125].
[156]R. Ch. Bokun, in: Second All-Union Conf. on Methods and Equipment for Research into the Coherent Interaction Between Radiation and Matter. Abstracts [in Russian], Institute of Atomic Energy, M., 1982, p. 77.
[157]A. L. Sharma, Alimuddin, and K. R. Reddy, Nuovo Cimento D **5**, 147 (1985).
[158]P. P. Kovalenko, V. G. Labushkin, E. R. Sarkisov, A. K. Ovsepyan, and I. G. Tolpekin, Prib. Tekh. Eksp. **29**, No. 3, 64 (1986). [Instrum. Exp. Tech. **29**, (3), 577 (1985)].
[159]B. Kolk, Phys. Lett. A **50**, 457 (1975).
[160]Shih Lin Chang, *Multiple Diffraction of X-Rays by Crystals*, Springer-Verlag, Berlin, 1985 [Russ. Transl., Mir, M., 1987].
[161]A. M. Afanas'ev and V. G. Kohn, Phys. Status Solid A **28**, 61 (1975); Acta Crystallogr. A **33**, 178 (1977).
[162]I. D. Feranchuk, Izv. Akad. Nauk BSSR Ser. Fiz.-Mat. Nauk No. 4, 109 (1981).
[163]S. A. Kshevetskiĭ *et al.*, Kristallografiya **30**, 468 (1985) [Sov. Phys. Crystallogr. **30**, 270 (1985)].
[164]H. J. Juretschke, Phys. Status Solid B **135**, 455 (1986).
[165]R. Colella, Z. Naturforsch. A **37**, 437 (1982).
[166]A. M. Egiazaryan and P. A. Bezirganyan, Izv. Akad. Nauk Arm. SSR Fiz. **14**, 261 (1979).
[167]S. A. Kshevetskiĭ, M. L. Kshevetskaya, *et al.*, Ukr. Fiz. Zh. **25**, 781 (1980).
[168]S. A. Kshevetskiĭ *et al.*, *ibid.* **31**, 1059 (1986).
[169]V. I. Kushnir *et al.*, Acta Crystallogr. A **41**, 17 (1985).
[170]V. A. Baskakov and B. Ya. Zel'dovich, Preprint FIAN SSSR No. 191 [in Russian], M., 1978.
[171]V. E. Dmitrienko and V. M. Kaganer, Metallofizika **9**, 71 (1987). [Phys. Met. (G.B.) (1987)].
[172]V. G. Baryshevskiĭ, Pis'ma Zh. Tekh. Fiz. **2**, 112 (1976) [Sov. Tech. Phys. Lett. **2**, 43 (1976)].
[173]M. A. Andreeva and S. F. Borisova, Kristallografiya **30**, 849 (1985) [Sov. Phys. Crystallogr. **30**, 493 (1985)].
[174]A. V. Andreev, Usp. Fiz. Nauk **145**, 113 (1985) [Sov. Phys. Usp. **28**, 70 (1985)].
[175]A. M. Afanas'ev, P. A. Aleksandrov, and R. M. Imamov, *X-Ray Structure Diagnostics in the Investigation of the Surfaces of Single Crystals* [in Russian], Nauka, M., 1986.
[176]M. Sauvage, C. Malgrange, and J. E. Petroff, J. Appl. Crystallogr. **16**, 14 (1983).
[177]E. A. Volkova, *Polarization Measurements* [in Russian], Izd.-vo. Standartov, M., 1974.
[178]J. Fischer *et al.*, Nucl. Instrum. Methods A **246**, 404 (1986).

Translated by S. Chomet[3)]